

Ecole Polytechnique
Promotion X2015
CONFAVREUX Basile



Graduate research internship report

A novel role for PiT1 and PiT2?

Biology department
Neurobiology

Teacher:
Dr Ego-Stengel

Directed by:
Dr Franck Oury
Dr Mariana Ramos-Brossier

April – August 2018

Institut Necker Enfants Malade
14 Rue Maria Helena Vieira da Silva
75993 Paris



Déclaration d'intégrité relative au plagiat

Je soussigné Basile CONFAVREUX certifie sur l'honneur :

1. Que les résultats décrits dans ce rapport sont l'aboutissement de mon travail.
2. Que je suis l'auteur de ce rapport.
3. Que je n'ai pas utilisé des sources ou résultats tiers sans clairement les citer et les référencer selon les règles bibliographiques préconisées.

Je déclare que ce travail ne peut être suspecté de plagiat.

Date : 8 juillet 2018

Signature :

RESUME / SUMMARY

Ce stage de 4 mois dans l'équipe du Dr Oury à l'Institut Necker Enfants Malades était une première expérience dans un laboratoire de recherche. Ce groupe étudie l'importance des facteurs circulants dans la régulation du développement et des fonctions cognitives du cerveau. Au cours de mon stage, je me suis plus particulièrement intéressé au rôle des co-transporteurs phosphate (cibles potentielles de nombreux facteurs hormonaux) dans la régulation des fonctions cognitives du cerveau.

Mon laboratoire d'accueil a récemment montré que parmi les co-transporteurs phosphate, seuls ceux de la classe III, PiT1 et PiT2, sont exprimés au sein du système nerveux central, suggérant un rôle important pour ces protéines transmembranaire dans cette région. Cependant, leurs rôles physiologiques au sein du cerveau restent encore inconnus.

Pour répondre à cette question, le laboratoire du Dr. Oury travaille sur le modèle murin, à la fois *in vivo* et *in vitro* (cultures primaires de neurones). J'ai eu l'opportunité lors de ce stage de caractériser et comparer les phénotypes de dérégulation de PiT1 et PiT2, *in vivo* et *in vitro*, et peut-être de découvrir un nouveau rôle pour ces protéines.

J'ai pu découvrir puis pratiquer les nombreuses techniques d'analyses moléculaires et cellulaires (Western Blot, PCR, qPCR, Immunofluorescence, Microscopie), mais aussi comportementales (Morris Water Maze, Novel Object Recognition, Contextual Fear Conditioning) effectuées en routine dans le laboratoire. Ce stage m'a aussi permis de développer des programmes d'analyses de tests comportementaux, et de mettre en pratique mes cours de vision par ordinateur reçu à l'Ecole. J'ai pu mesurer la nécessité et les nombreuses perspectives de l'informatique dans l'analyse d'expériences délicates comme le comportement.

This 4-month internship in Dr Oury's group at the Institut Necker Enfants Malade was my first experience in a research laboratory. This team explores the roles of circulating factors in regulating brain development and cognitive functions. I focused during my internship on two potential receptors for such factors: PiT1 and PiT2, type III phosphate transporters. It is well established that dysregulation of the inorganic phosphate Pi/Ca²⁺ homeostasis has important impact on neuronal survival and neurodegeneration. Pi transport in eukaryotic cells is mediated by sodium-dependent phosphate co-transporters (NaPiTs) such as PiT1 or PiT2.

Interestingly, my host laboratory demonstrates that PiT1 and PiT2, are the only NaPiTs expressed in the brain. Moreover, NaPiTs expression decline with aging in the brain. They also have been linked to numerous hormonal signalling pathways in other tissues. However, their functions in the central nervous system remain largely elusive.

Addressing this question, Dr. Oury's group demonstrate that PiT-1 and PiT-2 are abundantly expressed in hippocampus and that a selective hippocampal PiT-1 or PiT-2 down-regulation lead to memory impairments. Moreover, *in vitro* they showed that PiT-1 or PiT-2 down-regulation reduces the synaptic plasticity capacity in hippocampal neurons. Taken together, these data demonstrate an unexpected role of the NaPiTs in the brain, in regulating hippocampal-dependent memory functions and neuronal activities.

During my internship, I joined this project and I was introduced to all the different approaches of molecular and cellular biology developed in the lab (Western Blot, PCR, qPCR, Immunofluorescence, Microscopy), but also and mainly to the mouse behavioural analyses (Morris Water Maze, Novel Object Recognition, Contextual Conditioning). Moreover, I had the opportunity to develop programs to analyse behavioral tests, thus putting into practise the computer vision courses took at the Ecole Polytechnique. I witnessed how crucial Computer Science is and could imagine its numerous applications on delicate experiments such as behavioral analyses.

CONTENTS

| | |
|---|----|
| Déclaration d'intégrité relative au plagiat | 1 |
| Résumé / Summary | 2 |
| Contents | 3 |
| 1/ Introduction | 4 |
| 2/ Objectives: | 6 |
| 3/ Materials and methods..... | 7 |
| 3.1/ Primary hippocampal neuronal cultures..... | 7 |
| 3.2/ HEK293 cultures | 8 |
| 3.3/ Western-Blots..... | 8 |
| 3.4/ Immunofluorescence..... | 9 |
| 3.5/ Generation of mouse models of hippocampal PiT1 or PiT2 downregulation..... | 10 |
| 3.6/ Morris Water Maze (MWM) task | 10 |
| 4/ Results | 11 |
| 4.1/ In Vitro analysis of PiT1 or PiT2 downregulation | 11 |
| 4.2/ Effects of Pit1 or PiT2 downregulation in vivo:..... | 15 |
| 5/ Discussion | 17 |
| 6/ Conclusion..... | 18 |
| Appendix: Automated analysis of mouse behavioral tests..... | 19 |
| A1/ Context: hippocampus, neuronal plasticity and autophagy..... | 19 |
| A2/ Objectives:..... | 20 |
| A3/ Material and Methods | 21 |
| A4/ Results:..... | 22 |
| A5/ Discussion | 27 |
| A6/ Perspectives, work in progress | 27 |
| A7/ Weaknesses..... | 29 |
| A8/ Conclusion, perspectives: | 30 |
| Bibliography: | 31 |

1/ INTRODUCTION

PiT1 and PiT2 (SLC20, SLCa1, SLCa2) are transmembrane proteins of the SLC20 family, are its only family members in mammals. They are composed of respectively 652 and 679 amino acids, and are ubiquitously expressed in mammal tissues. Mice with mutated PiT1 die *in utero*. No PiT1 mutants have been found in human, probably since any not-silent mutation is lethal *in utero*. On the contrary, PiT2 mutants live and develop the Fahr disease. This autosomal dominant affection is characterized by rapid calcification of brain regions and Parkinson-like neurodegenerescence¹.

PiT1 and PiT2 have been described in the literature since the 90's as type III sodium-phosphate cotransporters. They share two homology domains spanning over 70 to 140 amino acid residues, which are referred to as PD001131. These domains were shown to be critical for phosphate transport^{2,3}.

Throughout the years, new functions have been discovered for these proteins in various tissues⁴. For instance, human PiT2 serves as a receptor for the amphotropic subgroup of gamma retroviruses (murine leukemia virus)⁵. A signalling role in cell proliferation, specific to PiT1 and independent from phosphate transport, was also discovered².

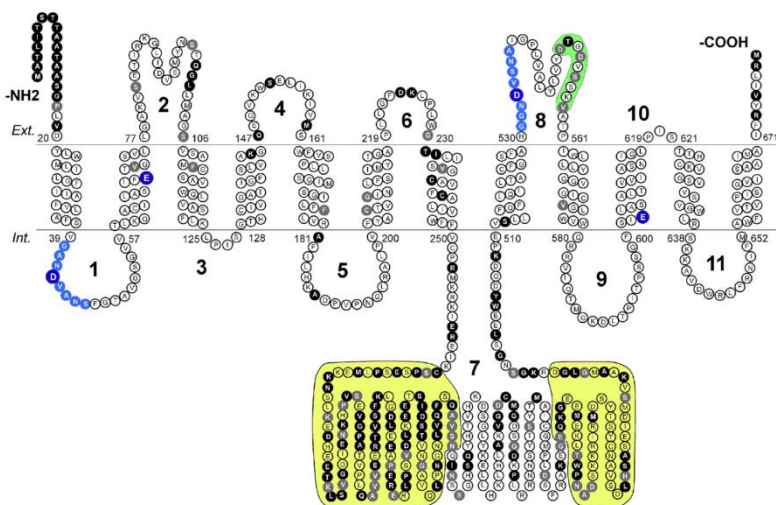


Figure 1: Topology of PiT1 and PiT2 (SLC20a1, Slc20a2) and the regions associated with their main functions known at this day. Sequences critical for phosphate transport are highlighted in blue. Light green shading indicates the region important for retroviral binding. Yellow shading indicates the regions that are not present in members of the PiT family from plants and bacteria.

For the last 20 years, numerous studies have underlined the importance of phosphate homeostasis, especially in the central nervous system⁶⁻⁸. A phosphocalcic deregulation can indeed have dramatic aftermaths on neuron survival and neurodegeneration⁹. However, the physiological role of phosphate and the signalling pathways involved are still to be discovered.

Therefore, our main objective is to understand the role of PiT1 and PiT2 in the brain.

Preliminary data from Dr Oury's group shows that PiT1 and PiT2 are ubiquitous phosphate transporter in the brain (fig 2). PiT1 and PiT2 are highly expressed in the brain compared to other regions, and are more abundant in the central nervous system than other known phosphate transporters.

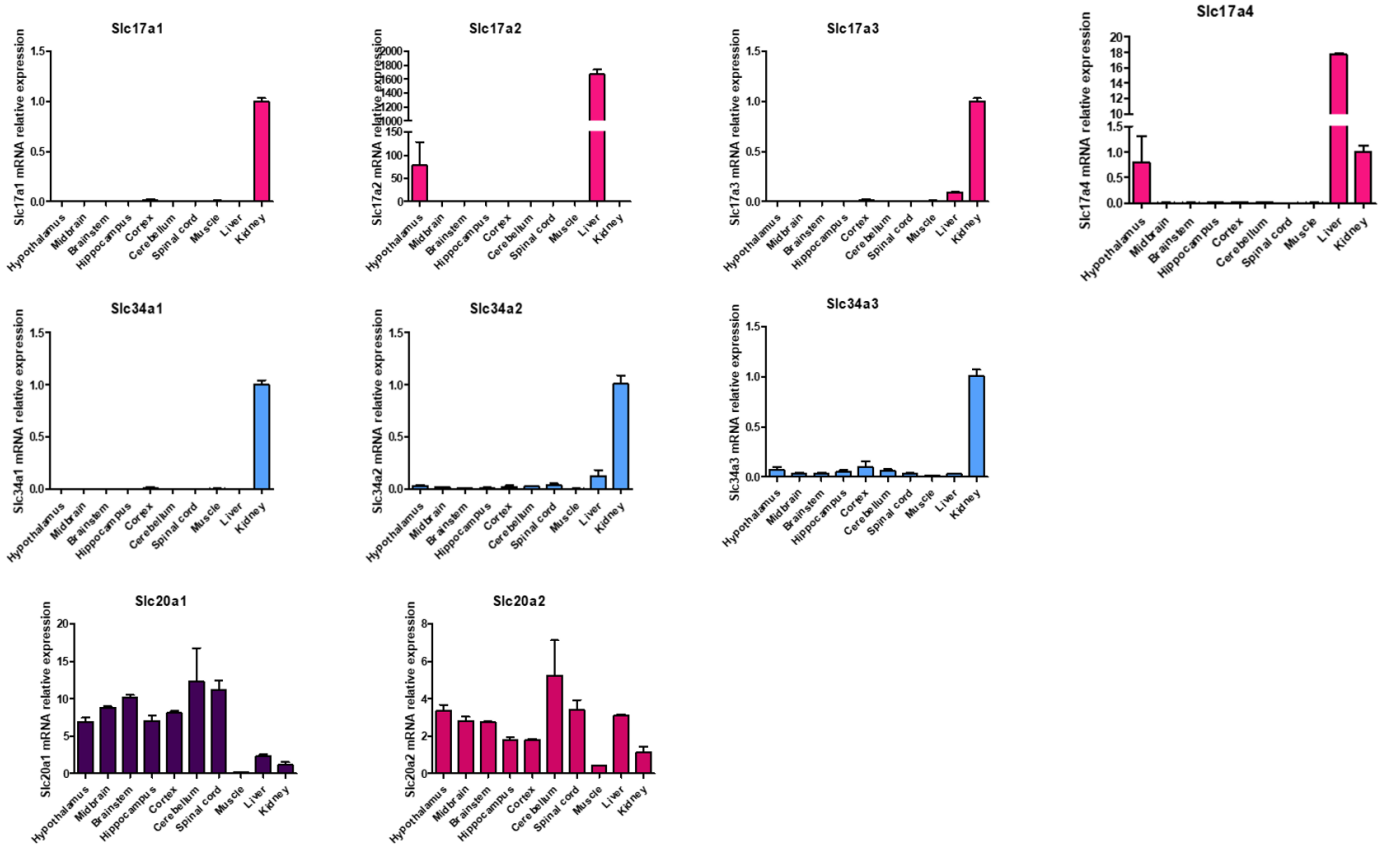


Figure 2: mRNA expression (relative to the kidney) of the *Slc34*, *Slc17* and *Slc20* families, the only SLC family members known to be phosphate co-transporters.

A morphological analysis was performed *in vitro* on primary hippocampal neurons. PiT1 and PiT2 were down-regulated using shRNAs. GFP (green fluorescent protein) was used to visualize neuronal morphology. Analysis of the dendritic branching (Sholl analysis, see 3.4.3/) leads to a clear phenotype. PiT1 downregulation generates neurons with less dendrites, whereas PiT2 downregulation creates neurons with less dendrites, closer to the soma on average (fig 3).

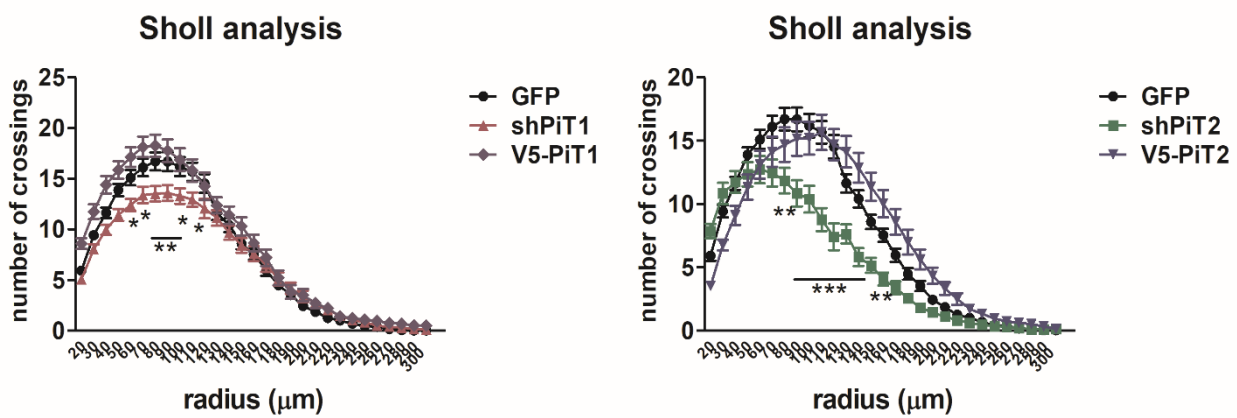


Figure 3: Sholl analysis of shPiT1,2 down regulated neurons or human PiT1,2 up regulated neurons. $n_{\text{Sholl}}(r)$ gives the number of dendrites present at a radius r of the soma.

Moreover, the Allen Brain Atlas highlights that specific brain regions show particularly high PiTs expression levels: CA3 and CA1 for PiT1; Hamon horn, CA3 and CA1 for PiT2. Since all these regions are part of the hippocampus, the choice was made to focus our study on this specific brain region.

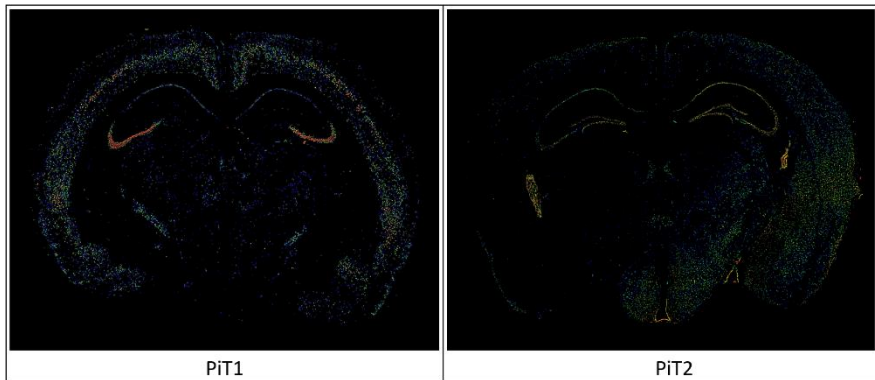


Figure 4: Allen Brain Atlas, In Situ Hybridization, coronal slice of mouse brain and the RNA expression of PiT1 (left) and PiT2 (right).

2/ OBJECTIVES:

To better understand the role of PiT1 and PiT2 in the brain, a first approach is to characterize the phenotype *in vitro* on primary hippocampal cultures. Once we observed an impact on the neuronal morphology, two main questions can be asked:

1. Determine if the morphological phenotypes after PiT1 and PiT2 inactivation are dependent on phosphate transport

1.1. Tools validation in HEK293 cells

1.2. Morphological study of the effect of transport-deficient mutant in neurons

2. Evaluate the impact of PiT1 and PiT2 inactivation for brain function

2.1. Assessing hippocampal-dependent memory using the Morris water maze

3/ MATERIALS AND METHODS

3.1/ Primary hippocampal neuronal cultures

3.1.1/ Isolation and culture conditions of primary hippocampal neurons

Hippocampi from C57 B6J 16 days embryos were dissected in L15 cold media. Neurons were dissociated chemically in Trypsine-EDTA 0,05% and mechanically by pipetting and then suspended in DMEM (Dulbecco's Modified Eagle Medium) supplemented with 10% foetal bovine serum, 1% penicillin/streptomycin. The dissociated cells were plated onto poly-L-lysine-coated twelve-well plates or onto glass coverslips in six-well plates for microscopic examination. Approximately 120 000 cells were placed in each well. On Day In Vitro 1 (DIV1), the medium was replaced with Neurobasal containing B27 supplement, Glutamax and Mycozap (complete neurobasal) and maintained until DIV18, time at which neurons are considered mature and used for transfection as presented below. The medium was changed by halves each week. Neurons were transfected at DIV11 with 600 ng of DNA using lipofectamine 2000 (Invitrogen), and fixed at DIV18.

3.1.2/ Primary hippocampal neurons downregulated for phosphate transport after transfection with shRNA-PiT1 or shRNA-PiT2

Genetic construction: To downregulate PiT1 or PiT2 in primary hippocampal neurons, we generated plasmids vectors containing a short hairpin RNA sequences targeting PiT1 or PiT2. The pSicoR plasmids were used. These plasmids are especially designed for shRNA, and contain GFP to check which neurons have been transfected.

The following sequence (sense-loop-antisense) was used for shRNA *PiT1*, the target sequence is highlighted:
5'-TCG AGC CGG CCC ATT GTA TTG TCG GTG CAA TTC AAG AGA TTG CAC CGA CAA TAC
AAT GGG TTT TTG C-3' (sense);
3'-GAT CCC AAA AAA CCC ATT GTA TTG TCG GTG CAA TCT CTT GAA TTG CAC CGA CAA TAC
AAT GGG CCG GC -5'(anti-sense).

And for shRNA Pit-2:

5'-TCC ACA GCT CAT CTT CCA GAA TTT CAA GAG AAT TCT GGA AGA TGA GCT GTG GTT TTT
TC-3' (sense);
3'-TCG AGA AAA AAC CAC AGC TCA TCT TCC AGA ATT CTC TTG AAA TTC TGG AAG ATG AGC
TGT GGA -5'(anti-sense).

As for the up-regulation of hPiT1,2 and their various mutated forms (mutants are described in the result section), PCDNA6 plasmids were used. These plasmids were kindly given to us by the Pr. Friedlander from I.N.E.M. They come with V5 and His tags.

Plasmid generation: As primary neuronal cultures are very fragile, we tried to generate plasmids with as few toxins and impurities as possible. As a result, we used the Endotoxin-free plasmid DNA purification kit from Macherey-Nagel, based on the NaOH/SDS lysis method from Birnboim and Doly¹⁰. All constructs were checked by Sanger sequencing

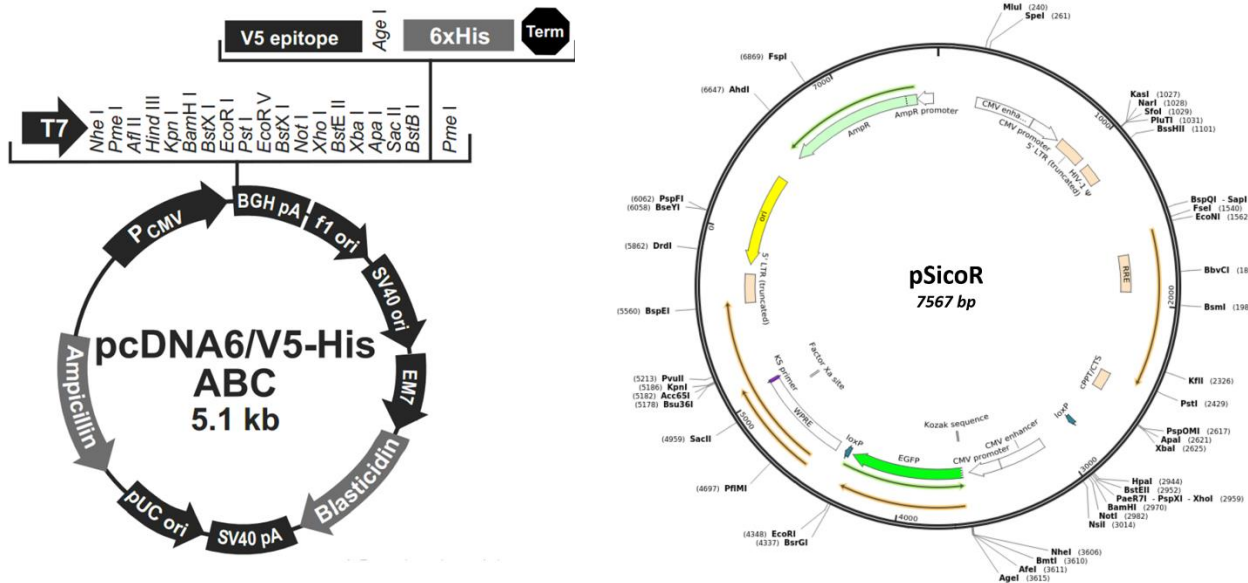


Figure 5: Map of the two plasmids used

3.2/ HEK293 cultures

HEK293 cells were cultured in DMEM media supplemented with 10% serum and penicillin/streptomycin. The HEK 293 culture was carried out according to the supplier's protocol (Invitrogen). Cells were plated onto poly-L-lysine-coated (1h, 37°C) twelve-well plates or onto glass coverslips. One day after plating, cells were transfected with 600 ng of DNA using lipofectamine 2000 (Invitrogen). 48h after transfection, cells were either lysed for protein extraction or fixed for immunofluorescence analysis.

3.3/ Western-Blots

Western blot analyses were performed on HEK293 cultures. Cells were rinsed in PBS 1X and proteins were extracted in Tris pH8 50mM, EDTA 1mM, EGTA 1mM, NaCl 200mM, SDS 1% and Roche® inhibitory cocktails 4%. Lysates were evaluated by Bradford. 20ug of protein were mixed with buffer 5,5X and DTT 1M and loaded on a 12,5% SDS polyacrylamide gradient gel and subsequently transferred onto a trans blot PVDF membrane (Biorad). Membranes were blocked in 5% BSA in Tris-buffered saline with Tween (TBST) and then incubated with either **rabbit anti human-PiT1** (1:500) from GeneTex (GTX105062), **rabbit anti human-PiT1** (1:500) from Proteintech (12423-1-AP), **rabbit anti human-PiT2** (1:500) from Proteintech (12820-1-AP) or **mouse anti-V5** (1:500) Invitrogen (R960-25) over night at 4°C, **mouse anti-βactin** (1:4000) from Sigma (A 5316) for 2hrs at room temperature. After several washes, blots were incubated in Horseradish peroxidase-conjugated secondary antibodies with 5% BSA for 45 min at room temperature and washed in TBST. ECL kit and Chemidoc apparatus were used to detect protein signals.

3.4/ Immunofluorescence

3.4.1/ Protocol

Neurons or HEK293 cells were first fixed in 4% PFA and 4% sucrose for 20 minutes at room temperature. Cell membranes were permeabilized with Triton 0,1%, PBS 1X for 15 minutes. Cells were incubated with 3% BSA in PBS with Tween (TBST) for 2h at room temperature and then incubated with either **anti human-PiT1** (1:500) from Genetex (GTX105062), **rabbit anti human-PiT1** (1:500) from Proteintech (12423-1-AP), **rabbit anti human-PiT2** (1:500) from Proteintech (12820-1-AP) or **mouse anti-V5** (1:500) Invitrogen (R960-25). After washing, cells were incubated with fluorophore-coupled secondary antibodies.

3.4.2/ Images

Images were taken with Zeiss Apotome using 20X objective.

3.4.3/ Morphological analysis (Sholl analysis)

Images were analysed using the ImageJ software, and its plugin Simple Neurite Tracer. A semi-automatic segmentation of dendrites was performed. Let r be the radius from the centre of the neuron's soma. The Sholl analysis consists in determining $n(r)$, the number of dendrites at a radius r from the centre of the soma. In other words, the number of intersections between the segmented neuron and a circle of radius r , centred on the soma. The scale of the analysis was set to 10 microns. Even when easily identifiable, the axon was counted as dendrite since in some cases, a clear distinction was impossible.

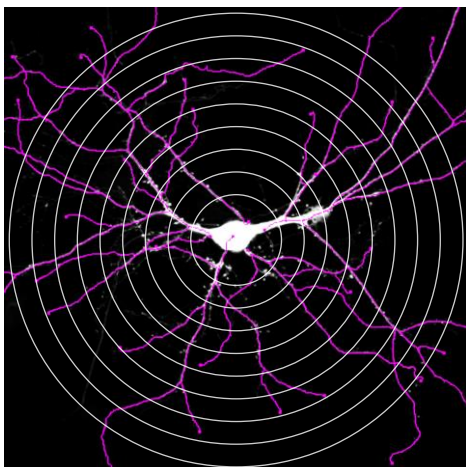


Figure 6: Illustration of the Sholl analysis for a given neuron, extracted from the ImageJ segmentation plugin. The dendrites and the axon selected for analysis are highlighted in magenta. The circles model the distance from the soma.

3.5/ Generation of mouse models of hippocampal PiT1 or PiT2 downregulation

A mouse model of a specific down-regulation of hippocampal PiT1,2 expression was generated by local stereotactic injections of genetic inhibitor. This model was obtained after local stereotaxic injections of Adeno-Associated- virus (AAV) expressing shRNA, targeting *PiT1* or *PiT2* (Vector).

Stereotactic injections in mice hippocampus: We used stereotactic injections to deliver AAV-shRNA-*PiT1,2* in mouse hippocampi. Surgical procedure: Mice were anesthetized by intraperitoneal injection of a mixture of ketamine and xylazine then placed inside the stereotactic instrument by adjusting the rods into the crevices just anterior to the animal's ears. An anterior-posterior incision was made and the tip of the needle, held by the stereotact to the bregma point at all three axes, was considered as the zero point (X=0; Y=0, Z=0). Next, we drilled a shallow hole, only in the skull bone using a fine driller at the following coordinates relative to bregma: anteroposterior (-2.0 mm) and mediolateral (± 1.4 mm) from the bregma. The needle was next moved to the correct location and inserted into the brain at -1.33 mm to the dorso/ventral axis from the brain surface (Paxinos Mouse Brain Atlas). The needle delivers 1 μ L per hemisphere of our molecule at a speed of 0,25 μ L/minute. Between each 1 μ L injected we wait for 4 minutes. Three weeks after injections, mice were tested for locomotor and anxiety phenotypes (open field and dark/light transition tests), and 3 different hippocampal-dependent memory tests: object location memory, contextual fear conditioning and Morris water maze (MWM). In this manuscript we will focus on the latter.

3.6/ Morris Water Maze (MWM) task

To determine an *in vivo* phenotype for PiT1,2 downregulation, mice were exposed to the MWM test. This test is widely used to study spatial memory and learning. Animals are placed in a pool of water that is coloured opaque with non-toxic tempera paint, where they must swim to a hidden escape platform. Because they are in opaque water, the animals cannot see the platform, and cannot rely on scent to find the escape route. Instead, they must rely on external/extra-maze cues. As the animals become more familiar with the task, they are able to find the platform more quickly. The test is divided into two phases: a 9-day training phase and a test phase on day 10.

During the learning stages (training), each animal was subjected to a daily four-trial session. Before the first trial of the first session (day 1), the mouse was placed for 30 sec on the platform then allowed to swim to reach the platform for a maximum period of 90 sec. Then, following this extra trial, the first session consisted of three trials placing the mouse in the pool, facing the wall of the tank. The mouse was allowed 120 sec to search for and climb onto the submerged platform. If the animal failed to locate the platform within this delay, it was subsequently placed on the platform by the experimenter. In all cases, the mouse was left on the platform for 5 sec. Then for the hidden platform training (day 2 to 9), each trial consisted of releasing the mouse into the water facing the outer edge of the pool at one of the cues (except the quadrant where the platform was located) and letting the animal swim to escape to the platform before 120 sec had elapsed. A trial terminated when the animal reached the platform, where it remained for 5 sec. The score of a mouse is the time taken to find the platform (120s if not found). For the test phase, the platform is removed and mice are left for 120 sec in the pool while a software records their position and speed in the pool. This trial is repeated four times on day 10. The software used was Anymaze. The pool is virtually divided into four quadrants. The platform's position is located at the centre of the first quadrant. The time spent in each quadrant is measured to determine if the mouse is searching for the platform.

4/ RESULTS

4.1/ *In Vitro* analysis of PiT1 or PiT2 downregulation

4.1.1/ Tools validation in HEK293 cells

Generation of plasmids: Plasmids contained shRNA against mouse *PiT1* or *PiT2*, human *PiT1*, human *PiT1* with a substitution at Serine 128 (S>A), human *PiT1* with a substitution at Serine 621 (S>A), human *PiT2*, human *PiT2* with a substitution at Serine 113 (S>A) and human *PiT2* Δloop, lacking a large intracellular loop (see fig 7, highlighted in yellow).

These constructs will be referred further as sh*PiT1*, sh*PiT2*, h*PiT1* WT, h*PiT1* S128A, h*PiT1* S621A, h*PiT2* WT, h*PiT2* S113A, h*PiT2* Δloop.

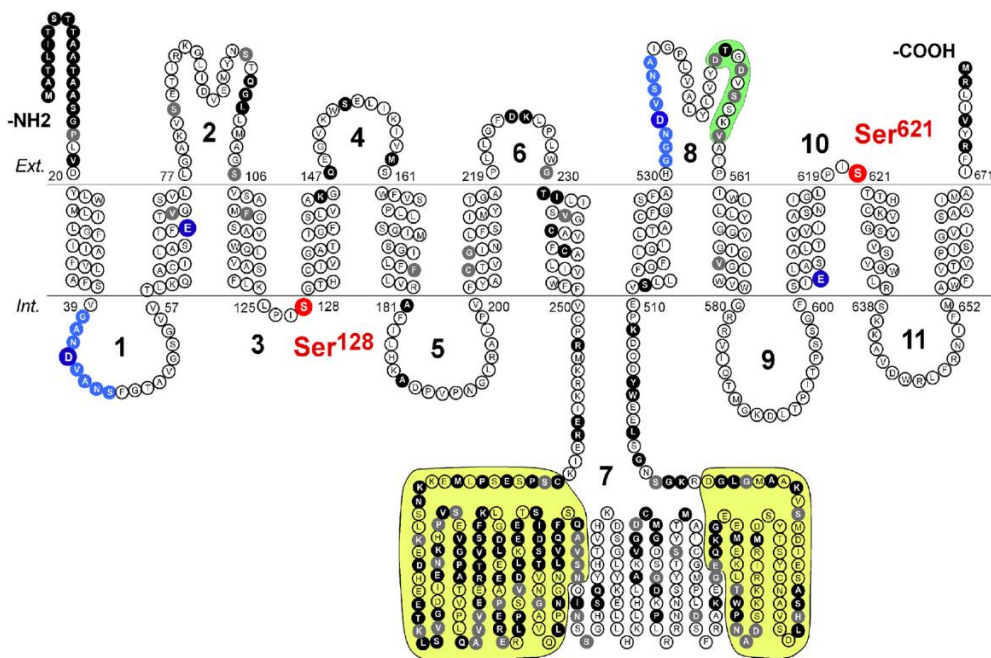


Figure 7: The *PiT1* sequence, like in the introduction, but the substitution sites have been highlighted in red.

These substitutions on the *PiT1,2* sequences were shown by a team of I.N.E.M. to hamper phosphate transport^{2,3}. As for *PiT2* Δloop, the entire intracellular loop has been removed (yellow on the above figure). This loop had been linked multiple times to signalling roles of *PiT2*³, and would therefore be a potential region for a new signalling role if phosphate transport isn't involved in these phenotypes.

Testing antibodies on HEK293: Different antibodies were tested on HEK cells. These cells are far more robust than primary neurons, and easy to transfect. For Pit-1 we tested three different antibodies: two rabbit anti-hPiT1 (from two companies) and mouse anti-V5. For Pit-2, rabbit anti-hPiT2 and mouse anti-V5 were used. The evaluation of the two antibodies was tested with two main criteria: first the ability of the antibodies to detect all the PiT1,2 mutants used in this study. Second the selectivity of the antibodies (their ability to interact with hPiT1,2 compared to endogenous mouse PiT1,2, or more anything else expressed at a basal level in the neurons). The objective is to be able to see as clearly as possible an overexpression of PiT1,2 in a neuron.

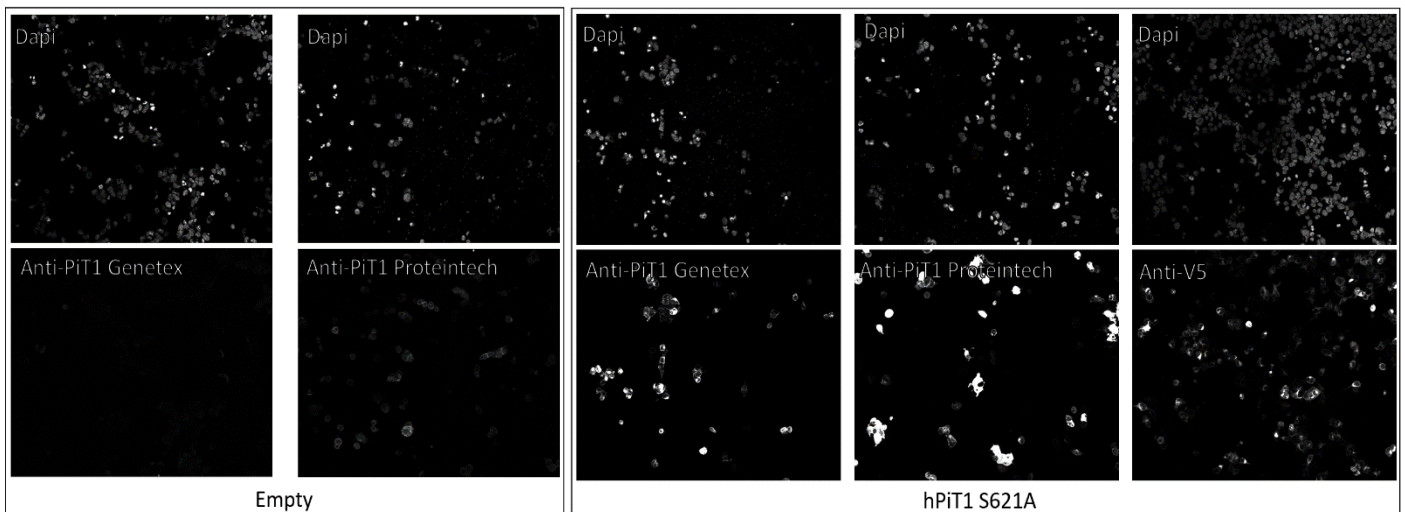


Figure 8: Photos from immunofluorescence for the candidate antibodies on the different PiT1 plasmids. On top the results for the wavelength corresponding to Dapi (nucleus), bottom the same area for the wavelength of the antibodies. Only a few results are shown here.

Proteintech seems all in all better to detect easily an over-expression (ratio $\frac{\text{overexpression luminosity}}{\text{background/endogenous luminosity}}$).

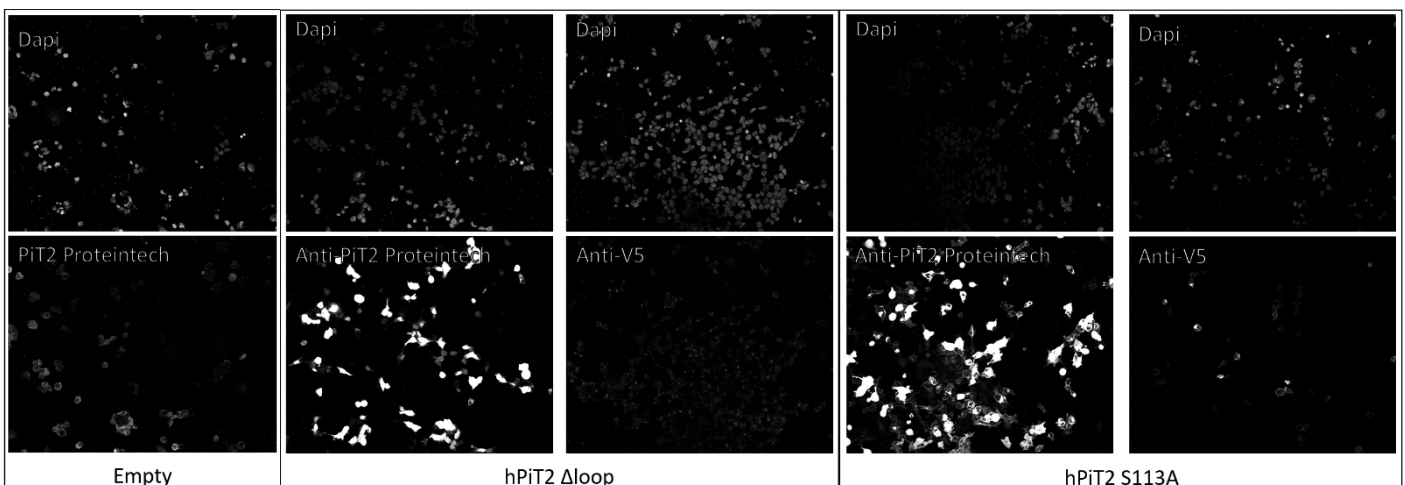


Figure 9: Photos from immunofluorescence for the candidate antibodies on the different PiT2 plasmids. The disposition is similar to the above figure for PiT1.

We observe that anti-V5 failed to recognise some plasmids such as hPiT2 Δloop and hPiT2 S113A.

Validation by Western Blot: To see if the plasmids indeed lead to a stable proteic expression and to confirm the results of the immunofluorescence performed above, Western Blots were performed on HEK293 cells transfected with the same conditions as for the immunofluorescence. In addition to the different PiTs wild type mutants, plasmid containing endogenous mouse PiT1 or PiT2 were transfected, to test further the antibodies specificity. With the anti V5 WB, we see that all mutated forms are present in comparable quantities, except Δloop. We also see that anti-V5 doesn't bind to endogenous PiT.

But with anti-PiT2, we have a large band for PiT2 Δloop. This means that Δloop is expressed and stable in HEK, but undetected by anti-V5.

What's more, no band appeared for PiT1 with anti-PiT1 Proteintech although β-actin is present. And as we saw with V5, PiT2 is expressed in the sample. This part should be done again to rule out any technical error. PiT have a glycosylation site, which may explain why the bands at 70kD are subdivided into two close bands. The bands seen at 130-140kD on the anti-PiT2 WB could be PiT1-PiT2, PiT2-PiT2 dimers. This dimerization had already been observed¹¹.

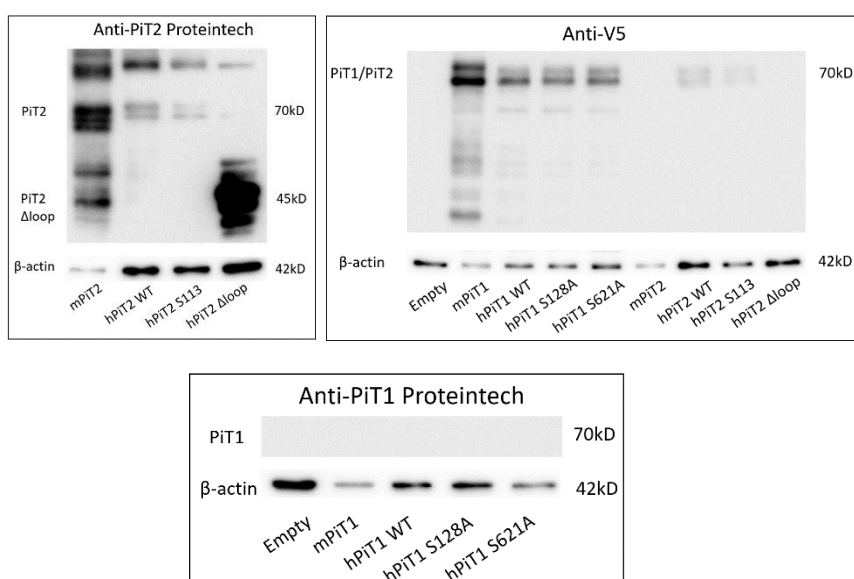


Figure 10: Western Blots of HEK293 cultures transfected with our series of plasmids. β-actin was used as normalisation. Empty was a plasmid containing GFP without V5 tag. Mouse PiT2 also had no V5 tag.

Anti-PiT1 from Proteintech was thus chosen over the two others for its high affinity with every mutant we had generated. Anti-PiT2 from Proteintech was thus selected, by default since V5 was unable to detect two mutated forms of PiT2.

Testing different co-transfection ratios: A first attempt of co-transfection (shPiT1,2 + PiT1,2/mutants) on primary neurons was made, with the team's usual conditions. However, no co-transfection was seen. We thus decided to test different co-transfection factors on HEK293 cells. This time, HEK were co-transfected with pSicoR-empty (the plasmid which will be used with shRNA) and hPiT1. We haven't checked with PiT2 or the mutants as their size are similar and we are only trying to optimize the entry of both plasmids in the cell. We tried different co-transfection ratio, $r = \frac{n_{pSicoR-empty}}{n_{PCDNA6-hPiT1}}$. Other parameters such as $n_{tot\ plasmids}$ or the different quantities of reagents to optimize the transfection had already been optimized in previous experiments on primary neurons.

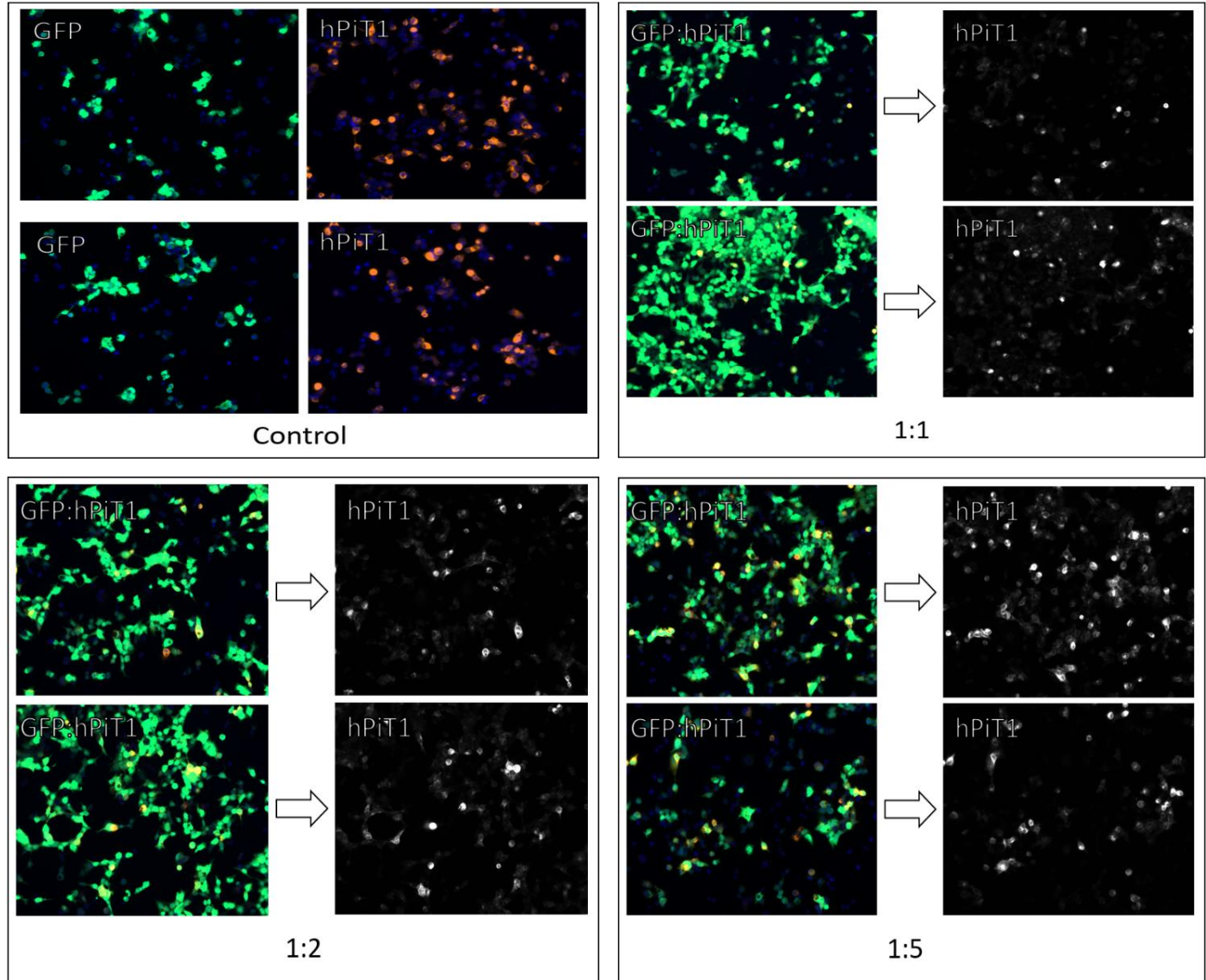


Figure 11: Photos taken with fluorescence microscopy (Objective 20X) after an immunofluorescence on HEK cells transfected with pSicoR-empty plasmids (GFP, green) and/or PCDNA6 plasmids with hPiT1 WT (orange). The DAPI is in magenta (nucleus). Two photos for each condition are shown. On the left a merged image of the three wavelength is presented. On the right only anti-hPiT1 are shown.

We observe that the pSicoR plasmid easily transfects cells whereas PCDNA6 transfects far less cells. There are clearly two conflicting influences for the choice of r : the more pSicoR, the more cells transfected, but the more pSicoR, the less cells transfected by GFP. Indeed, the total number of plasmid injected per well on neurons has an upper bound, otherwise the culture rapidly dies from the stress induced (chain reaction). As a result, we chose to keep the 1:5 ratio, which appeared to generate the most co-transfected cells.

4.1.2/ Rescue experiment on PiT1,2 downregulated primary hippocampal neurons:

We downregulated mouse PiT1 or PiT2 in mice primary hippocampal neurons, while inducing an over expression of human PiT1, PiT2 or different mutants. These mutants were shown unable to transport phosphate while leaving the structure of the protein unchanged (and hopefully their other roles as well)^{2,3}. Cultures were observed by immunofluorescence. We used the antibodies and the co-transfection ratios described in the previous parts, and had synthetized the plasmids carefully, checked their sequence and purity. Nevertheless, no co-transfection was seen.

However, shPiT2 controls were used to confirm the morphological phenotype described in the preliminary results. Although fewer neurons were counted in this case (24 in total) than for the preliminary result, we observe a significative difference in the distribution: shPiT2 neurons possess less dendrites, distributed closer to the soma.

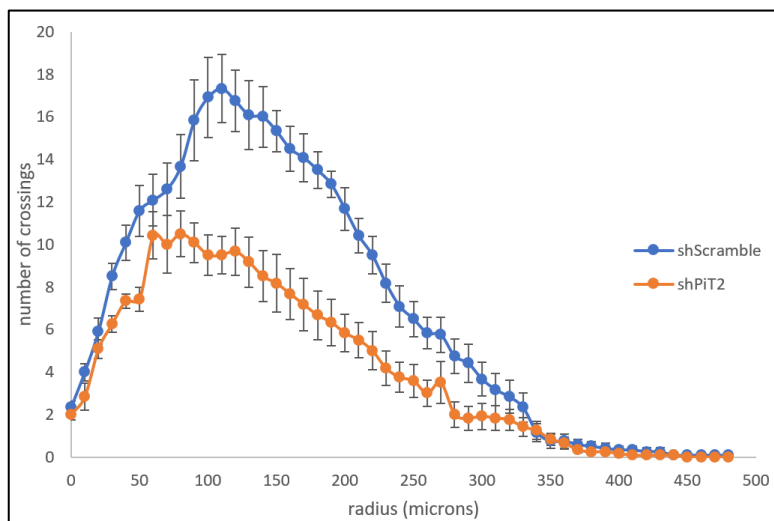


Figure 12: Sholl analysis on primary neurons transfected with shPiT2 or shScramble. Two cultures were analysed for each condition, $n_{shPiT2}=12$, $n_{shScramble}=12$.

For PiT2, the phenotype is obvious. Dendrites are almost absent in shPiT2 neurons. Axons, however, don't seem to be affected in the same way by the absence of PiT2.

4.2/ Effects of Pit1 or Pit2 downregulation *in vivo*:

4.2.1/ Tool validation

Other team members injected mice with AAV containing shRNA against PiT1 or PiT2 in the hippocampus, and checked the expression of mRNA by qPCR. Their results highlight a 60% decrease in the expression of PiT1 and PiT2 RNA. This decrease goes along with an increase for the other protein, hinting at a possible complementation between PiT1 and PiT2.

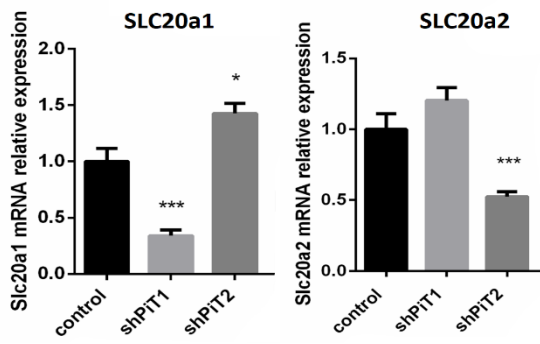


Figure 13 : Quantitative PCR on hippocampal RNA ($n_1=4$ (PiT1), $n_2=4$ (PiT2))

4.2.2/ Effect of specific downregulation of PiT1 and PiT2 in the brain on cognitive functions

To determine the functional consequences of a selective PiT1 or PiT2 downregulation in the hippocampal region of the brain, we generated a cohort of 3 groups of mice ($n=10$ per group) that were previously injected specifically in the hippocampus with either shPiT1, shPiT2 or shScramble (control group).

The cohort was then subjected to the Morris Water Maze task in order to characterize the spatial hippocampal-dependent memory. This test assesses the ability of mice to use spatial cues to locate a hidden platform during 9 successive days. We observed a significant delay in spatial learning and memory capacities after hippocampal down-regulation of either PiT-1 or PiT-2, in comparison to control group (Figure 14, left panel). This was confirmed by a probe trial 24h after the last day of acquisition. It consisted in letting the mouse swim for a fixed duration (120 sec). The platform was removed but cues on the walls remained. The performance was expressed as the time spent in the target quadrant where the platform was located during the hidden platform training. We observed here less preference for the target pool quadrant in shPiT1 or shPiT2 groups as compared to control group (AAV-shRNA-Scramble) (Figure 14, right panel). Importantly, no modifications were observed for the speed or the distance travel during the probe trial MWM task within the different group of mice. Taken together, these results demonstrate that PiT1 and PiT2 are required in hippocampus to control hippocampal-dependent learning and memory.

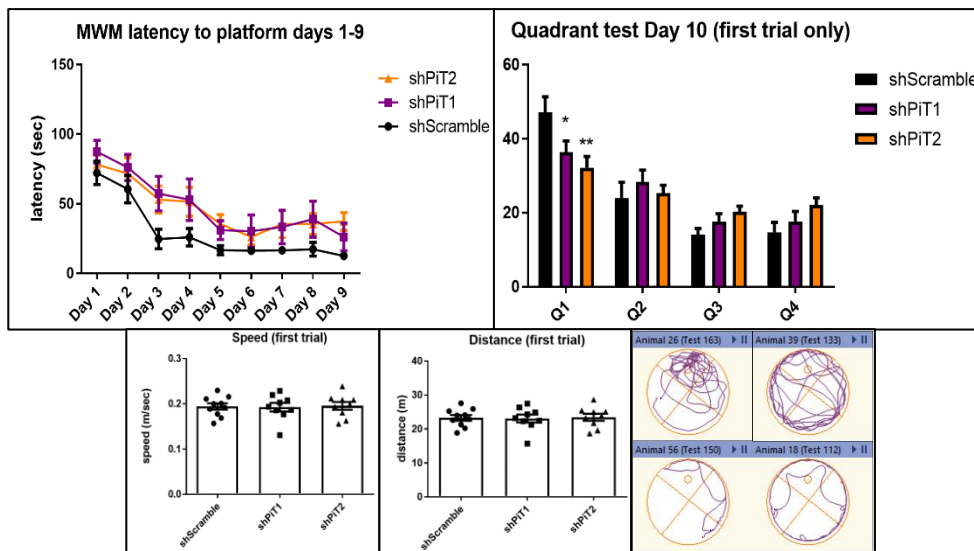


Figure 14: Top: Results of the Morris Water Maze training phase (day 1 -> 9. The mean of the 4 trials of each day are counted). Middle: Results for day 10 test phase. The pool is divided into four quadrants, the platform being at the centre of Q1. Bottom: Locomotive control of the three groups at the first trial at day 10, and trajectories of 4 mice in the test phase. Note: mouse 13 (shPiT1, “animal 56”) and 21 (shPiT2, “animal 18”) were excluded from the analysis since they showed no will to swim at all. This is confirmed by their day 10 trajectory (bottom right).

5/ DISCUSSION

Our data suggests that downregulation of PiT1 and PiT2 in neurons induces important morphological deficits in primary hippocampal neurons. Indeed, we have observed that Pit1 or PiT2 downregulated neurons possess less dendrites, closer on average to the soma. These *in vitro* observations are consistent with the previously described neurodegenerescence phenotypes present in Fahr syndrome patients. However, our main goal to determine the independence of this phenotype to phosphate transport remains unanswered, although the experiment is still ongoing.

Our *in vivo* analyses demonstrate that downregulated selectively PiT1 or PiT2 in the hippocampal region of the brain lead to important spatial learning and memory deficits as demonstrated in the Morris Water Maze task and probe trial task.

The primarily goal of our *in vitro* analyses was to investigate whether the cellular phenotype observed after downregulation of PiT1 or PiT2 in neurons is dependent or not on the role of PiT1 and/or PiT2 in phosphate transport. To that end, we wanted to test whether diminution in dendritic spine density and branching observed after in primary neurons after downregulation of PiT1 or PiT2, can be rescue after over expression of WT human PiT1, PiT2 or different mutants unable to transport phosphate (while leaving the protein conformation unchanged^{2,3}). Indeed, if the phenotype can be rescued by WT form of human PiT1 or 2, but not by the mutants for the phosphate transport, it would suggest that the role of PiT1 and/or PiT2 in hippocampal neurons is dependent on its/their actions in phosphate transport. Conversely, if both forms of PiT1 and/or PiT2 reverse this morphological phenotype in primary hippocampal neurons, it would indicate that their roles in regulating neuronal plasticity are independent on their functions in phosphate transport and would hint at a new signalling role of the class III co-transporter in neurons. In this perspective, the mutant PiT2 Δloop was added in the analysis. This intra-cellular loop is indeed a mammalian specificity and a key region of many signalling roles discovered for PiT2 independent of phosphate transport.

Comments on the *in vitro* experiment: We first validated our plasmid constructs and transfection protocols in HEK293 cells. We next performed several attempts for this rescue experiment on primary hippocampal neuronal cultures. Unfortunately, very few cultures survived and did not provide enough data to be presented in this manuscript. Several possibilities may explain this problem:

- The plasmid and their products are toxic for the neurons. However, numerous co-transfections on primary neurons using the same backbones were performed in the past by the lab without such issues.
- We performed all our preliminary set up on HEK293 cells. These cells are known to be very easily transfected, robust, less sensitive to environmental changes in comparison to primary neuronal cultures. The numerous cell deaths we encountered suggest that other parameters to optimize cell survivability must also be considered. In our case, a single plasmid with both the shRNA and PiT would allow us to bypass this delicate transfection step, and probably perform better. Adjustments using several other plasmid ratios needs to be tested as well.
- Primary neurons are known to be extremely fragile and sensitive to O₂/Co₂ changes. Unfortunately, the lab was during my presence in temporary premises, and shared its cell culture room and incubators with other groups. The multiplication of experimenters in this room may explain their high mortality during these few months (a problem that was already observed in the past). This possibility is the most likely since we are currently repeating this experiment in another cell culture room without such issues.

Comments on the *in vivo* experiment: To reinforce our results, we will repeat the behavioral analyses in additional cohorts of mice downregulated for PiT1 or PiT2 selectively in hippocampal neurons (currently on going). Cohorts will also undergo other behavioral tasks assessing hippocampal-dependent memory such as Novel Object Location, Contextual Fear Conditioning and Novel Object Recognition. Indeed, one behavioral test alone cannot characterize correctly a phenotype. Unmeasured factors have a dramatic influence on mice's performance (period of the year, smell, size of the experimenter, presence of works in the nearby road...¹²). Moreover, the measures we take (latency or time spent in each quadrant for the MWM) are very basic compared to the complexity of the behaviour of an individual. As an experimenter of the Morris Water Maze, I witnessed situations where a mouse had clearly understood where the platform was and how to use the signs to find its orientation. But it had also understood that it would be put back in the water a few minutes later, no matter what. Another mouse was swimming in circles, without a clue about why it was there. Both behaviours were scored in the same way: a latency to find the platform of 120s. To what extent is this number representative of the reality of the test? This is why before throwing any conclusions, a wide variety of tests, each of them testing a particular aspect of memory, must be undergone on large number of mice, multiple times. Only by this mean can an average effect on behaviour be drawn.

Lastly, PiT1 and PT2 expression in the brain is not restricted to hippocampus. Indeed, in the future the phenotypic investigation of PiT1 or PiT2 downregulation in the central nervous system may be also developed for other part of the brain, such as the hypothalamic region (region of the brain exhibiting the highest level of expression of PiT1 and PiT2 after the hippocampus) and their potential role in regulating the hypothalamic control of energy metabolism.

6/ CONCLUSION

This work suggests that PiT1 and PiT2 have important roles in the brain. We are slowly starting to associate the topology of this multifaceted PiT family with its numerous functions. We have validated the phenotype *in vitro* of PiT1 and PiT2 downregulated neurons. Our results also demonstrate that morphologic changes observed *in vitro* could lead to impairments in cognitive functions *in vivo*.

* If the *in vitro* phenotype is linked to phosphate transport, it would provide one more evidence of the quintessential importance of phosphate homeostasis in the central nervous system, and could hint at one more research direction on numerous CNS diseases such as Parkinson or Alzheimer.

* If the *in vitro* phenotype appears to be independent of phosphate transport, a new pathway awaits further research. Which molecules could interact with PiT1 or PiT2, how does this pathway influence cognitive functions? A shortlist of potential interactors with PiT1 and PiT2 has already been drawn.

Our *in vivo* analyses exhibit the same behavioural phenotype after selective downregulation of either PiT1 or PiT2 in the hippocampal region of the brain. This observation could suggest that PiT1 and PiT2 have a synergistic role in neuron and behaviour, or that both molecules are involved in the control of different neuronal functions (morphology, survival, proliferation, excitability...) but their inactivation will lead to the same behavioral phenotype.

If the two molecules have the same role in neuronal cells, it would fit with the phosphate transport possibility, since the same domains critical for phosphate transport are present in the two proteins. This complementation could be also suggested by the fact that shPiT1 injections lead to an increase of RNA PiT2 expression and reciprocally (as seen in fig 10). However, such complementation, if it exists, is incomplete since the phenotype we observed *in vitro* for the PiT1 or PiT2 down regulations were very different. Therefore, the molecular mode of action of each PiT need to be investigate so as to determine their respective mode of action on neurons.

APPENDIX: AUTOMATED ANALYSIS OF MOUSE BEHAVIORAL TESTS

A1/ Context: hippocampus, neuronal plasticity and autophagy

Hippocampus and age-related memory deficits: In the mammalian brain, learning and memory rely on neuronal structural reorganization and plasticity of the hippocampus. The hippocampus is also the most commonly affected brain region by aging, which leads to learning deficits and memory impairments^{13,14}. With increased life expectancies in developed societies, the number of individuals affected by age-related memory loss is bound to dramatically increase. However, normal brain aging is a complex and multifactorial process, influenced by both genetics and environmental factors. Therefore, identification of cellular mechanisms favoring hippocampal-dependent memory and neuronal plasticity is of utmost importance. Among the variety of intracellular mechanisms, my host laboratory shed light on the physiological role of autophagy in the hippocampal region of the brain.

Autophagy: Autophagy is a highly conserved catabolic process leading to the degradation of macromolecules and organelles by the lysosome. Here, we will focus on macro-autophagy (which we will hereafter refer to as autophagy). Autophagy is initiated by the formation of a double-membraned surrounded vacuole: the autophagosome (see fig16). The biogenesis of autophagosome is orchestrated by multiple signaling pathways and dynamic membrane complexes containing Autophagy-related proteins (ATG), such as Beclin-1, ATG14, Vps34, that are essential for the formation of double membrane autophagosomes. The ATG5/12/16L1 complex finally allows for the lipidation of the LC3 protein (LC3II) which is then recruited to the site(s) of nascent autophagosome to favor the growing of the double membrane structure and its maturation¹⁵.

Basal autophagy has a function in neuronal homeostasis, playing a role in pre- and post-synaptic assembly, dendritic spine pruning, axonal growth and dopamine release. Emerging evidence also supports roles for autophagy in synaptic plasticity¹³. In the brain, the housekeeping role of autophagy has been extensively studied in the context of neurodegenerative diseases, such as Alzheimer's.

Beyond its basal functions, autophagy can be also stimulated to regulate tissue homeostasis by mediating cellular adaptive stress-responses to various physiological stimuli and changes in environmental conditions. Importantly, multiple reports indicate that ATG proteins expression is reduced in aged tissues, including brain in which Atg5, Atg7 and Beclin 1 (Becn 1) are found to be downregulated¹⁶. However, the physiological role of autophagy in the regulation of cognitive functions remains elusive.

Autophagy influences memory formation and synaptic plasticity: Dr. Oury's group has recently observed that mouse hippocampal region exhibits the highest level of autophagic flux and ATGs proteins expression in the brain and that stimulating memory by exposing mice to various behavioral tasks up-regulates autophagosome formation in the hippocampal neurons. Based on these observations and knowing that the formation of novel memories requires changes in neuronal protein synthesis/degradation and organelle turnover, the laboratory started to investigate a possible physiological role of autophagy in the hippocampus region of the brain for the regulation of memory functions.

Using hippocampal injections of genetic and pharmacological modulators of autophagy, they found that inducing hippocampal autophagy is necessary to form novel memory, by modulating the adaptive neuronal response to novel stimuli. Mechanistically, they show that autophagy induction is necessary in shaping activity-dependent pre-synaptic plasticity in hippocampal neurons. Taken together, this series of data reveals that inducing autophagy in hippocampal neurons is a necessary mechanism to enhance the integration of novel stimulations of memory by modulating pre-synaptic plasticity, which include increased dendritic spine formation and neuronal excitability. Moreover, they also demonstrate that hippocampal autophagy is reduced during aging and that restoring its level can restore age-related memory decline. They showed that autophagy is necessary to mediate the recently described beneficial effects of young blood-derived factors on memory decline in aged-mice. Their results reveal the importance of promoting hippocampal autophagy in mediating the adaptive responses of neurons to novel memory stimulations and humoral factors showing the potential therapeutic benefits of modulating autophagy in the brain to reverse the effects of aging on cognitive functions.

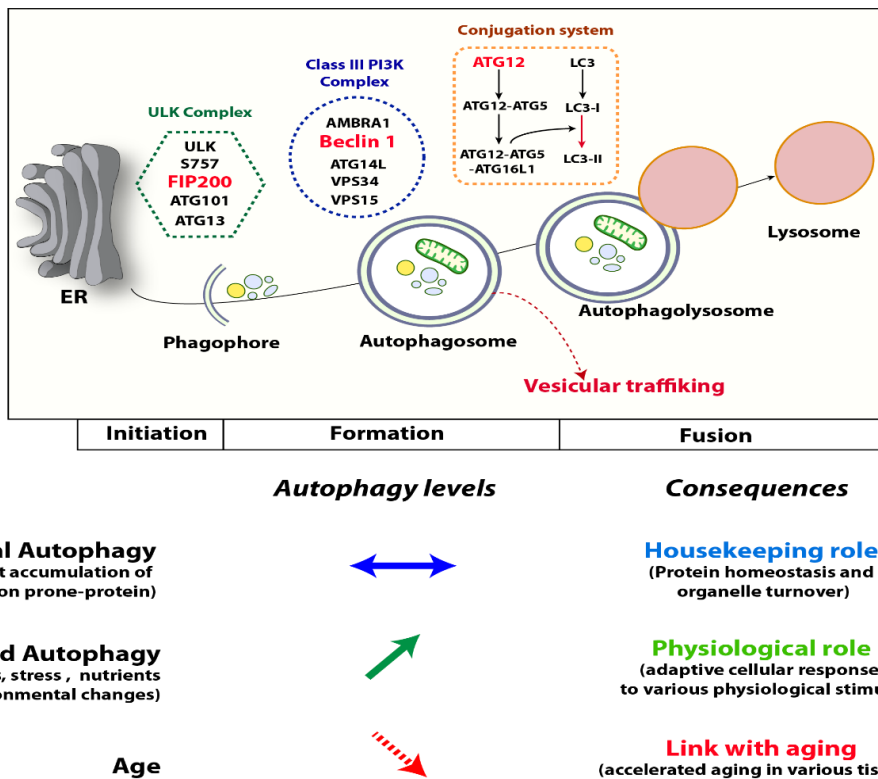


Figure 15: The process of autophagy in mammalian cells, and its key machinery players

A2/ Objectives:

Following this study, Dr Oury's group submitted a paper (currently in revision) describing their major findings. However, several comments were issued on this manuscript by the reviewers:

* The first point is whether autophagy selectively in neuron is involved in this process. Indeed, Dr. Oury's laboratory had generated various mouse models to selectively downregulate hippocampal autophagy by performing stereotactic injections of adeno-associated viruses (AAV) expressing shRNAs against various ATGs of the autophagy machinery. Mice underwent various behavioral tests, among which the Novel Object Recognition task (NOR, see fig16). However, this strategy was not discriminative. Indeed, the shRNA inserted in AAV is under control of an ubiquitous promoter, and is thus expressed in all hippocampal cell types: neurons but also astrocytes, glial cells, oligodendrocytes...

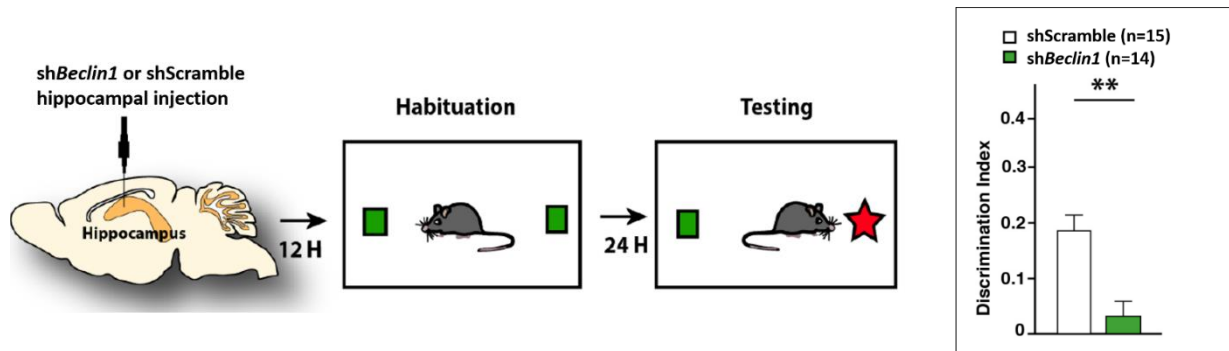


Figure 16: NOR test on a batch of mice injected with either shScramble (no target sequence in the mouse genome) or shBeclin1 (shRNA targeting Beclin-1 protein necessary in the initiation of the autophagy process). A Student test was performed on the discrimination index of the two groups, leading to a p-value < 0,001.

* The second point discussed was the potential effect of downregulation of hippocampal autophagy on the locomotor activity, that can introduce a bias in their interpretation of the behavioral analysis in NOR. Even though the team had been careful about such parameters using other behavioral tests to assess locomotion, they had not quantified the mice's locomotion directly in NOR. This was a broader remark concerning all the mice subjected to behavioral tests in the paper.

Therefore, one axis of my master internship was to pursue the investigation of this important role of hippocampal autophagy in regulating memory formation and brain aging. To that end, I contributed to the work in addressing these two important questions:

Aim1- To determine whether selective neuronal hippocampal downregulation of autophagy influences memory formation

Aim2- To test and develop a software for the systematic analysis of the locomotor activity in several mouse models of hippocampal autophagy downregulation

A3/ Material and Methods

A mouse model of selective hippocampal neuronal downregulation of *Beclin1* was generated, by performing local stereotactic injections of Adeno-Associated- virus (AAV) expressing shRNA selectively targeting our gene of interest.

Hippocampal Stereotactic injections:

See Material and Method for the PiT project

Viral vectors: Adeno-associated viruses (AAV) expressing shRNA were purchased from Vector Biosystems Inc (Malvern PA). We used an AAV expressing shRNAmir targeting *Beclin1* (Becn 1) specifically in neuronal cells (AAV9-eSYN-GFP-*Beclin1*-shRNAmir) (named in the figures: AAV-eSYN-*Beclin1*-shRNAmir) that were purchased from Vector Biosystems Inc (Malvern PA). *Beclin1* shRNAmir is driven by the eSYN promoter, a hybrid promoter consisting of the 0,45Kb human Synapsin 1 promoter fragment (hSYN1). AAV-eSYN-GFP-shRNA155mir was used as a control. These constructs will therefore be referred as eSYN-sh*Beclin1* and eSYN-shScramble. For both AAV, we have injected 1ml (bilaterally) of viral solution, 3 weeks prior to behavioral tests or brain tissue collection. The AAV titers were between 2.8 and 4.3×10^{13} GC/ml.

Behavioral Tasks:

To assess the functional role of autophagy in regulating hippocampal-dependent memory, we subjected our mouse models to a behavioral task assessing predominantly hippocampal-dependent memory and known to be altered by aging.

Novel object recognition and location (NOR): The Novel Object Recognition test (NOR) assesses the rodent's ability to recognize a novel object in the environment and consisted of three phases: habituation phase, a training phase, and a testing phase.

Habituation phase: On the first day, mice were habituated to the arena, where they were allowed to explore the apparatus for 5 min and then were taken back to their home cage.

Training phase: On the second day, mice were allowed to explore two identical objects arranged in a symmetric position from the centre of the arena, for 10 min. The animals returned to their home cage.

Testing phase: After 24 hours, mice were tested in the same arena to explore two objects: a familiar object and a novel object. One of the previously explored objects was placed in the same location as in the training phase while the second familiar object was replaced by a novel object. Mice were allowed to explore both objects for 15 min. As a note, for each phase, mice will be placed in the centre of the arena at the start of each exposure. All behaviour sessions were recorded with a video camera affixed to a tripod above the testing arena.

Video analysis: Behaviour is scored on videos by two observers blind to treatment and the total exploration time of the objects is quantified in the testing phases. Object investigation will be defined as orientation of the head toward the object with the nose within 1 cm of the object. Investigation will not be scored if the mouse will be on top of the object or completely immobile. The animal memory performances are evaluated by measuring the discrimination index: $d = \frac{\text{exploration time}_{\text{novel object}} - \text{exploration time}_{\text{familiar object}}}{\text{exploration time}_{\text{novel object}} + \text{exploration time}_{\text{familiar object}}}$

A4/ Results:

Aim1: To determine whether selective neuronal hippocampal downregulation of autophagy influence memory formation

It was decided to change the promoter in the shBeclin-1 plasmid. From an ubiquitous promoter, the team decided to test the the *synapsin 1* gene hybrid promoter. This protein is a member of the synapsin family known to regulate neurotransmitters at synapses¹⁷. Its promoter was shown to generate expression in neurons only, with high specificity¹⁸. Thus, by coupling the precise localization of stereotactic hippocampal injection and the specificity of the *synapsin 1* promoter, we should be able to express sh*Beclin1* selectively in hippocampal neurons.

Other team members thus injected 20 mice with either eSYN-shScramble or eSYN-sh*Beclin1*. Of note, both AAV expressed EGFP that allowed them to confirm the site of stereotactic injection and infection efficacy by visual examination of EGFP expression on brain coronal sections by fluorescence microscopy. LC3 Immunofluorescence (Scale bar = 20 μ m) was performed by other team members on hippocampal cross-sections, at the level of the dentate gyrus (DG), CA3 and CA1 of 3-month-old mice previously injected with either AAV-eSYN- Beclin 1 shRNAmir or AAV-eSYN- Scramble-shRNAmir. As a result, they observed that the LC3 puncta present in the various hippocampal region of the brain were drastically reduced after injection with the AAV-eSYN- Beclin 1 shRNAmir in comparison to the control mice (AAV-eSYN- Scramble-shRNAmir).

Mice then underwent the NOR test. We observe a significative variation of discrimination index in the same sense as with the previous sh*Beclin1*. This assesses that neuronal autophagy is indeed responsible for the memory loss observed in Dr. Oury's preliminary experiment with sh*Beclin1* under the ubiquitous promoter.

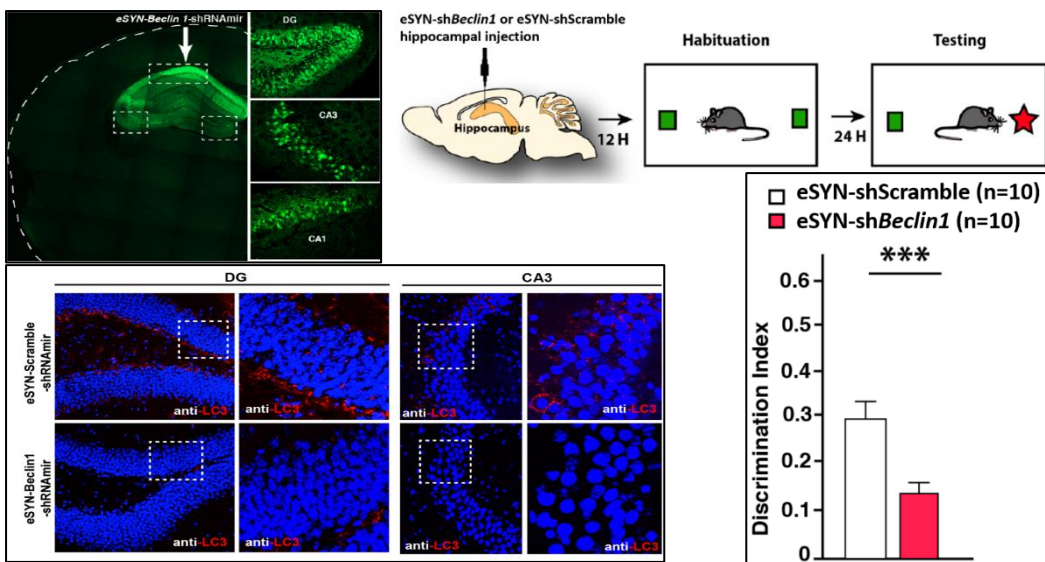


Figure 17: Mice injected with eSYN-shBeclin1 or eSYN-shScramble specifically in the hippocampus, and their results in the testing phase of the Novel Object Recognition test (left). A Student test was performed on the discrimination indexes of the two groups, the p-value was < 0,0001. The injection site and the number of infected cells were verified (plasmids expressed eGFP). A LC3 immunofluorescence was performed (LC3 is a marker for autophagy) in both Scramble and shBeclin mice.

Aim2- To test and develop a software for the systematic analysis of the locomotor activity in several mouse models of hippocampal autophagy downregulation

Constraints: The concerned batches spread on a two-year range, for a total of over 500 mice, all already sacrificed. But the videos used to quantify the exploration time of the mice remained. A 15 minutes film of the mice's actions in a container was at our disposal. But how to quantify a mouse's locomotion? The most natural answer is via their mean speed, which boils down to the distance covered in a given amount of time. The human eye being unable to quantify the distance covered, an automatic analysis was mandatory. However, these videos weren't recorded for an automated analysis perspective: almost everything varied from one batch to another: the number of cages, the luminosity, the framing... No affordable software on the market would accept such entries, as they are often coupled with a precise setup.

The final object-oriented program runs on Python 3 (Anaconda base distribution + OpenCv). The code is accessible on GitHub (see bibliography for code). The main constraint around this algorithm is its execution time: with 15 frames per second, 15 minutes per mice, 500 mice, over 100 000 images must be computed on a basic computer. As a result, it was impossible to use OpenCv segmentation tools, or navigate through the entire image at each frame. Moreover, mice have irregular movements, so analysing a fraction of the frame would lead to a biased result. The algorithm is thus as local as possible and uses multithreading.

Algorithm's outlines: The starting hypothesis of this tracking algorithm is that the mouse's position on the next frame is close to its position on the current frame.

Let f_n be the n^{th} frame:

Once f_n is segmented, we hopefully get a convex subset S_n of f_n , representing the mouse's position in f_n . Here, as the mouse is dark and the rest is lighter, the segmentation is a simple thresholding on the intensity of the pixel. The threshold depends on the video and is chosen by the user.

Let b_{n-1} be the mouse's barycentre found for f_{n-1} , we search for b_n :

- If $b_{n-1} \notin S_n$, the mouse can't be far from b_{n-1} . A local search starting from this point enables us to find $b'_{n-1} \in S_n$, an arbitrary pixel of the mouse.

- If $b_{n-1} \in S_n$, $b'_{n-1} = b_{n-1}$.

We can now compute b_n , starting from b_{n-1} (process described in the figure below).

The distance covered $dparc$ is then actualised: $dparc = dparc + ||b_{n-1}b_n||$, so is the grid (object detailed in the following part).



Figure 18: Iterative algorithm to find the barycentre of a convex subset. A search in the 8 cardinal directions is launched and stops at the border of the subset. The barycentre of the 8 border points will be the new starting point. This algorithm has very low spatial and temporal complexity, and in practice converges in under 5 iterations.

The Grid: Grid is an object which divides the container into 12 zones and measures the number of crosses between the mouse's trajectory and this fictive grid. This method was used by biologists in the past (by adding a grid in front of their screen!). It seemed important to us to have different quantifications of the distance covered to validate the algorithm. However, after a few tests, it appeared that the total number of grid crosses was heavily dependent on the initialisation of the container by the user, as explained in the figure below.

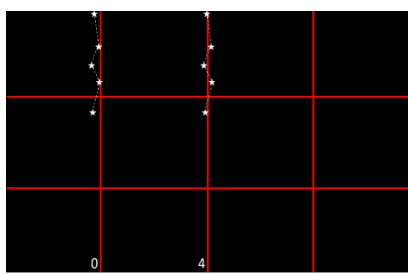


Figure 19: A few pixels difference in the initialisation can lead to major variability for a given trajectory. The same trajectory with a few pixels offset with respect to the vertical lines of the grid is drawn. On the left, the mouse will be added 0 grid crosses and in the middle 4. This is an undesirable bias since the distance covered is of course the same for the two trajectories. In practice, as mice often have erratic movements, such situations often happen and the resulting grid crosses depend on how the user defined the container limits at the beginning of the analysis.

Therefore, the choice was made to replace the grid's lines by stripes as shown below.

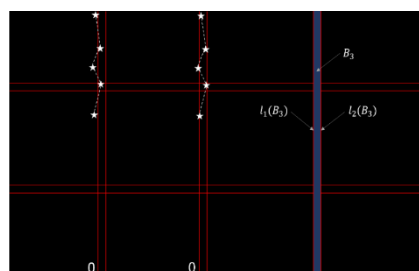


Figure 20: The transformation of lines in stripes eliminates these variations with erratic movements close to the lines. The width of the grid was set to 1cm.

However, now the Grid object needed a memory matrix to check if the mouse had entered a stripe and from which side.

| | | | | |
|---|-------|-------|-------|----------------|
| | 0 | 1 | 0 | |
| 0 | | | | False False |
| 0 | | | | False False |
| | False | False | False | False |

Figure 21: Representation of the Grid object. We can see the number of crossings with each stripe of the grid, and 2 booleans associated with each stripe to know if the mouse had entered the corresponding stripe, and from which side.

The algorithm checking if there is a collision with any of the stripes are tests on scalar and vector products (2D video games collision algorithms).



Figure 22: The grid drawn on a frame to analyse (left), the blue star is the old barycentre. On the right the segmented image and the actualised barycentre (blue star).

Architecture:

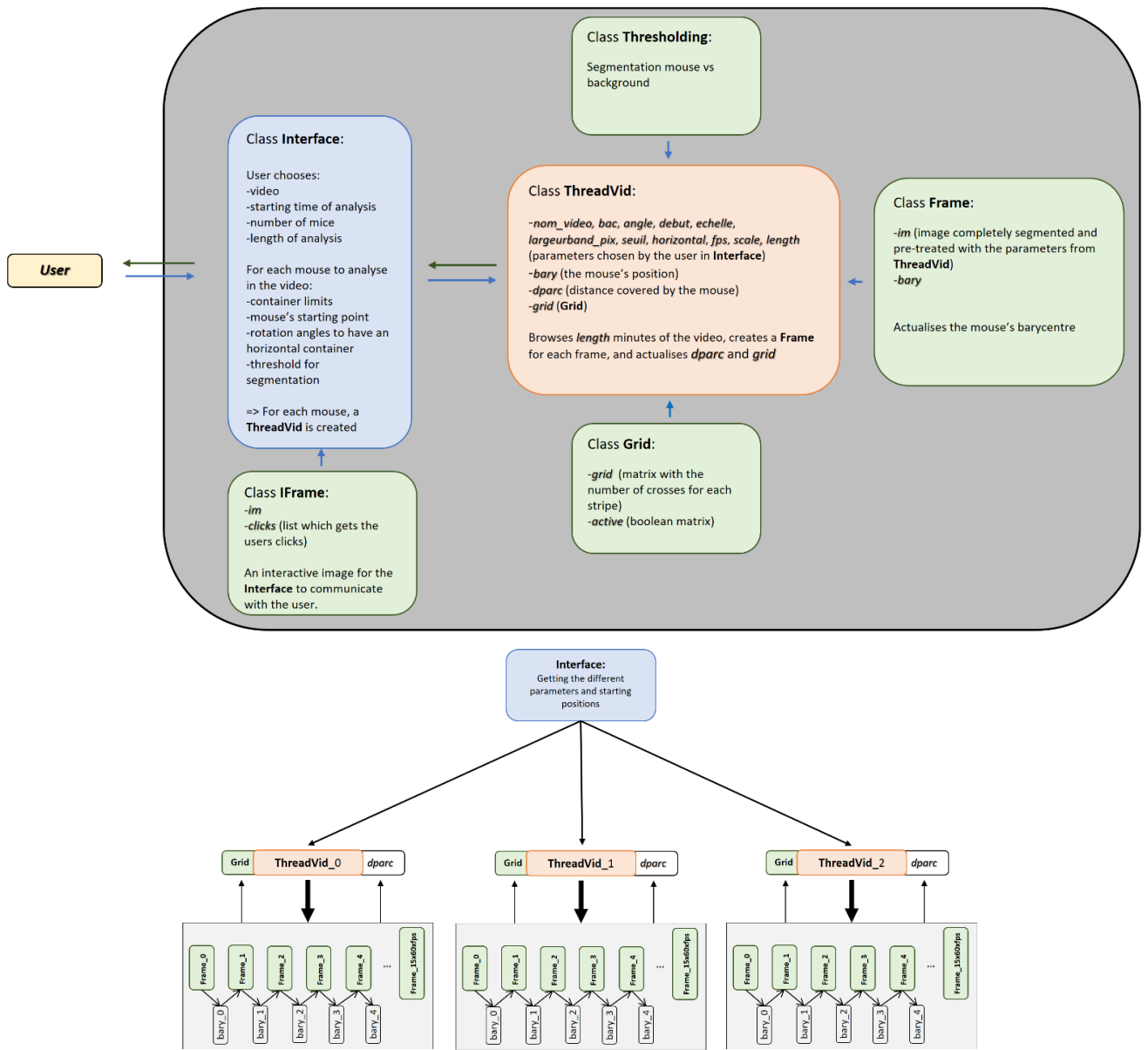


Figure 24: The algorithm in action on three mice

Results: The results obtained were analysed with the Prism software for statistical analysis (Student tests, or one-way ANOVA if more than one group) and graph generation.

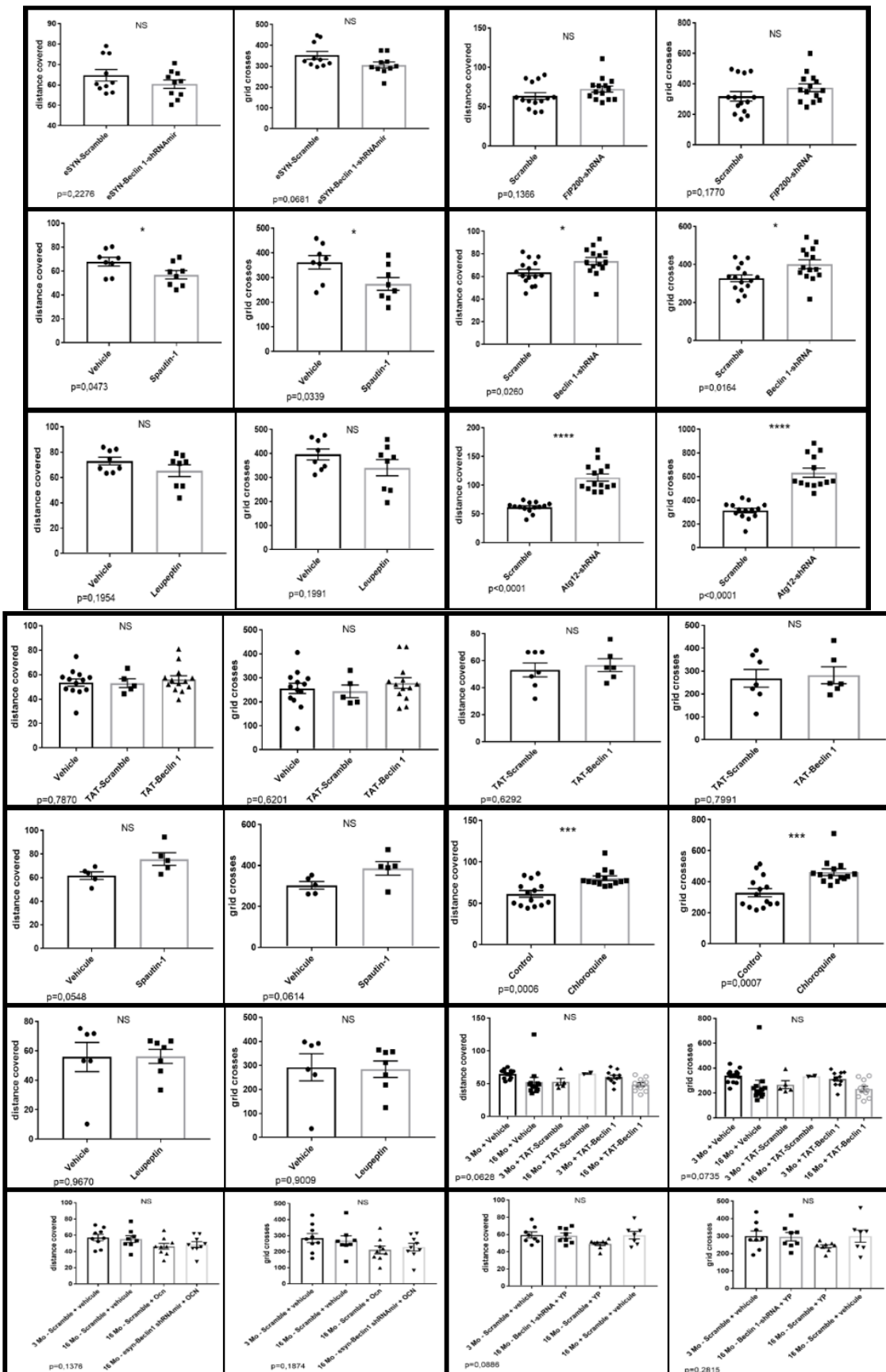


Figure 25: Locomotion tests of the batches used in the paper submitted. For each experiment, the two measures of distance are represented side by side. Student tests (or one-way Anova if more than two groups) were performed.

A5/ Discussion

Neuronal hippocampal downregulation of Beclin1: Our data suggests that the downregulation of *Beclin1* in hippocampal neurons leads to a decrease in NOR test performance. This downregulation has the same effect as a broader *Beclin1* downregulation concerning all hippocampal cells. We have thus confirmed that hippocampal neuronal autophagy is responsible for the memory loss observed in downregulated mice.

Locomotion control: We were able to use the video recording to assess control locomotion. To begin with, we can see that the two measures for motricity are very coherent with one another: if there is a variation between groups, it is always in the same sense with the same significance for both measures. Another validity check for this algorithm is that 3 months mice are more active than 15 months mice. This is the case in most results. Moreover, only four experiences show a significative difference in locomotion: ATG12, Chloroquine, Spautin, and sh*Beclin*.

As far as ATG12 and Chloroquine are concerned, there is an undeniable locomotor difference. Experimenters had noted a hyperactivity of the injected mice compared to the control ones, and shared these observations in the paper. This program confirms and quantifies these remarks.

However, results for Spautin and sh*Beclin*, labelled as significative, have to be nuanced:

Spautin: The p-value of the Student test is very close to the 95% threshold. We also observe high intra-group variability compared to the mean difference between the two groups. Moreover, the second batch analysed shows no significative difference, and a trend in the other sense than the first batch.

sh*Beclin1*: The batch of eSYN-sh*Beclin1* shows no significative difference and a trend in the other sense as for sh*Beclin1*, even though they had received, promoter excluded, the same construct. Moreover, we have shown before that from a behavioral point of view there was no difference between the two batches.

Therefore, the strong memory-related results obtained by Dr. Oury's lab cannot be put into question from a locomotion point of view.

A6/ Perspectives, work in progress

Analysing behaviour in the Novel Object Recognition task: From this program, the natural follow-up was the development of a real software which could analyse mice behaviour by deciding when mice were exploring an object. Keeping the core classes and general architecture of the locomotion algorithm, a few things were to be added:

- A better description of the mouse, which can't be reduced to its barycentre now we need to distinguish whether it is exploring the object or not.
- A new way to actualise the mouse's information from one frame to another.
- A way to decide whether the mouse is exploring or not.
- A Graphical User Interface to make the algorithm usable by anybody.

New description of the mouse: The mouse is now described by 3 points: its head, its barycentre and its tails. Two ways to actualise the mouse's descriptors were developed:

Mouse actualisation process (long): The same nomenclature as in the previous part will be used.

We start by actualising the barycentre in the same fashion as in the locomotion program to obtain b_n .

We find $e_{n1} \in S_n$ such as $e_{n1} = \underset{e \in S_n}{\operatorname{argmax}}(distance(e, b_n))$, the furthest point of the mouse from b_n .

We compute $e_{n2} \in S_n$ such as $e_{n2} = \underset{e \in S_n}{\operatorname{argmax}}(\operatorname{distance}(e, e_{n1}))$, the furthest point of the mouse from e_{n1} .

The algorithm to find e_{n1} and e_{n2} is described in the figure below. The Euclidian distance was used.

Hypothesis: e_{n1} and e_{n2} are the head and the tail of the mouse, but we don't know which is which. This is well verified in practise.

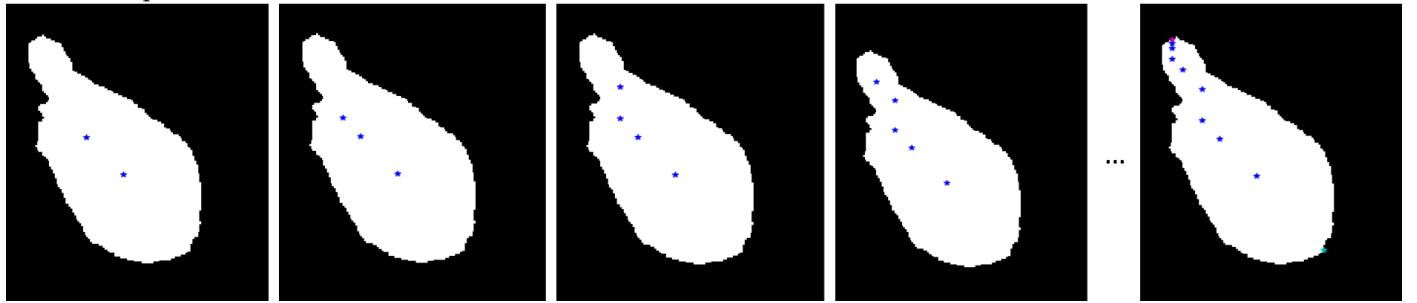


Figure 26: To find the furthest point on the mouse from the barycentre, we use a local search. We explore the 8 cardinal directions, and select the one which leads the furthest, and select the middle of that segment (left picture). A new exploration is launched in the two adjacent directions to the one we selected previously. The middle of the longest segment is selected. We then repeat this last step. In practise, in under 5 iterations, this method converges to an appropriate point, even for odd mouse shapes like the one represented.

We will then mark as tail the point (among e_{n1} and e_{n2}) which is closest to the widest part of the mouse. We indeed observed that the mouse's rear legs-torso junction was the widest part of its silhouette.

We thus navigate through the perpendiculars of $[e_{n1}, b_n]$ and $[e_{n2}, b_n]$, which we assume represent the width of the mouse. (process described in the figure below).

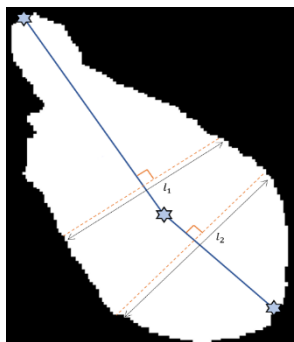


Figure 27: Finding which extreme point is the tail. l_1 and l_2 are first computed. They are the maximum width of the mouse on $[e_{n1}, b_n]$ and $[e_{n2}, b_n]$. The extreme point closest to the widest perpendicular will be labelled as the tail, and the other as the tail.

Mouse actualisation process (short): The two extreme points are found as explained in the previous paragraph. But we label as tail the point closest to the tail found in the precedent frame. This is cheap to compute and introduces a dose of continuity in the tracking. But in practise, this method must be checked from time to time with the long actualisation version since switches may happen.

Exploration: We chose to label the mouse as exploring an object (assimilated to a disk \mathcal{C}) if:

- Its head was less than 1cm away from \mathcal{C}
- Its barycentre is not inside \mathcal{C} (otherwise it had escalated it to try to escape the cage and is not exploring)
- The ray $[b_n, \text{head}_n]$ intersects \mathcal{C} . This is a way to assess that the mouse is looking at the object.

The GUI is under development, and the validity of the algorithm has to be checked. However, first tests are encouraging: the mouse is correctly segmented, the computed head and tail correspond to the real head and tail, and the exploration conditions implemented match with the reality.

A7 / Weaknesses

Program improvements: The programs developed or in development in this part are far less potent than numerous professional offers on the market. However, given the time allowed to run the analysis, and the fact that the videos at our disposal were incompatible with usual automatic analysis, we had no other immediate choices. The program could use improvements, like trying to detect the tail by machine learning on a smaller image centred around the barycentre. Since we don't have a large training set, transfer learning might be a possibility to explore.

General interpretation of behavioral tests: Important variability is encountered in behavioural tests, even for same age mice from identical lineage. This can be illustrated with the sh*Beclin1* and eSYN-sh*Beclin1* experiments described before. If we a Student test is performed without precaution on the two control groups (same age, lineage, treatment, protocol, two months apart), we find out that the two controls are “significantly” different from one another. This means that two groups from two different batches cannot compose a single population (in the sense used for the Student test). Too many unmeasured parameters and conditions may vary in these very sensible tests (period of the year, experimenter, intra cages social events, past social life...), giving birth to significant differences. If we regroup batches with one another, the hypothesis that individuals are chosen randomly among the population is wrong. Nevertheless, behavioral tests must be run on numerous mice, multiple times, to carry any sense, but have to be statistically analysed and interpreted with caution, as it is performed by my host lab. However, in our case, the question was to decide whether or not significative results in memory tests could be invalidated by locomotion control. We were able to provide a sure answer (no).

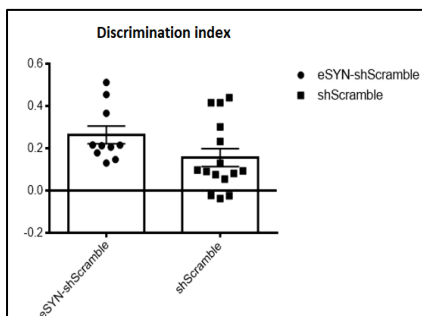
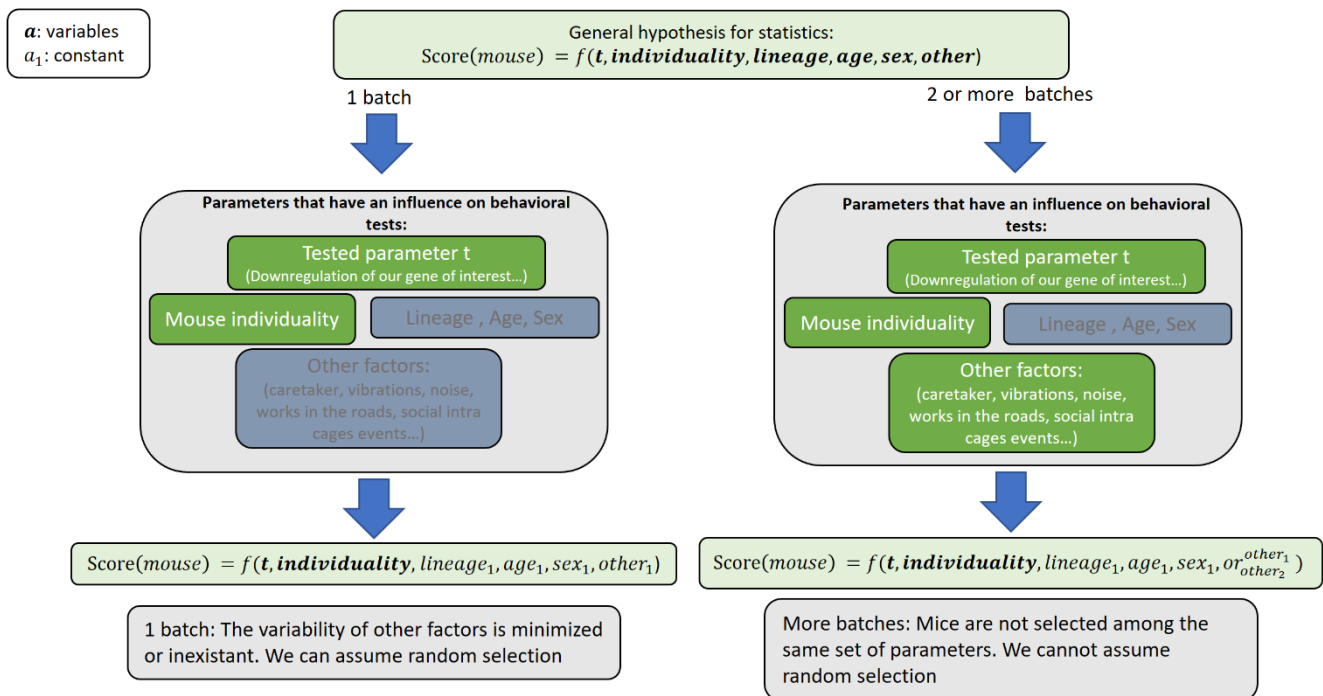


Figure 28: Comparison of the discrimination index between controls from two experiments: eSYN-shScramble and shScramble mice. The mice had undergone rigorously the same protocol at a few months interval. This doesn't carry any sense biologically, it points out the variability of behaviour and the need for an informed interpretation of such tests.

A8/ Conclusion, perspectives:

Addressing the critics made on Dr Oury's paper allowed us to precise the effect of hippocampal neuronal autophagy on mouse behaviour. This confirms the team's intuition that autophagy is all but a background process, a key to understanding learning and aging. Indeed, we provide here the demonstration, using AAV expressing shRNA driven by a neuronal promoter that the crucial role of hippocampal autophagy in controlling novel memory formation and synaptic plasticity in the brain, is dependent, at least in part, on the autophagic activity in "neuronal cells".

On the Computer Science side, a program able to reliably measure a mouse's distance covered was developed, and a more elaborate one describing mice's behaviour is under test phase. The specificity of this computer vision problem (easy segmentation, faster than real time analysis required) led us to develop an original tracking tool, although, at this day, it needs the help of more advanced Computer Science techniques. This was a first approach on the delicate analysis of behavioral tests, and I was alerted on the difficulty to study behaviour and the necessity to update the traditional tests, the parameters monitored and their analysis.

Dr Oury's laboratory has demonstrated the crucial role of autophagy in the hippocampal region of the brain for the control of memory formation by modulating neuronal plasticity. However, they did not explain how autophagy influences neuronal plasticity. It is now crucial to investigate this aspect.

We can emphasize several angles of attack to tackle this important question:

- Determine the autophagosomal proteome profiling after memory stimulation.
- Study the autophagosome dynamic and localization in hippocampal neurons after memory stimulation.
- Define the impact of up- or down-regulation of autophagy on receptor trafficking and synaptic plasticity in stimulated hippocampal neurons.
- Determine the neurotransmitter contents and release after up- or down-regulation of autophagy in hippocampal neurons

BIBLIOGRAPHY:

1. Saleem, S. *et al.* Fahr's syndrome: literature review of current evidence. *Orphanet J. Rare Dis.* **8**, 156 (2013).
2. Beck, L. *et al.* Identification of a Novel Function of PiT1 Critical for Cell Proliferation and Independent of Its Phosphate Transport Activity * □ S □. (2009). doi:10.1074/jbc.M109.053132
3. Salaü, C., Rie, V., Chal, M. & Heard, J. M. Transport-deficient Pit2 Phosphate Transporters Still Modify Cell Surface Oligomers Structure in Response to Inorganic Phosphate. doi:10.1016/j.jmb.2004.04.050
4. Sugita, A. *et al.* Cellular ATP synthesis mediated by type III sodium-dependent phosphate transporter Pit-1 is critical to chondrogenesis. *J. Biol. Chem.* **286**, 3094–103 (2011).
5. Sala, C., Rodrigues, P. & Heard, J. M. Transmembrane Topology of PiT-2, a Phosphate Transporter-Retrovirus Receptor. *J. Virol.* **75**, 5584–5592 (2001).
6. Abraham, K. A., Brault, J. J. & Terjung, R. L. Phosphate uptake and PiT-1 protein expression in rat skeletal muscle. *Am. J. Physiol. Physiol.* **287**, C73–C78 (2004).
7. Shaker, J. L. & Deftos, L. *Calcium and Phosphate Homeostasis. Endotext* (MDText.com, Inc., 2000).
8. Lederer, E. & Miyamoto, K. Clinical consequences of mutations in sodium phosphate cotransporters. *Clin. J. Am. Soc. Nephrol.* **7**, 1179–87 (2012).
9. Landfield, P. W., Applegate, M. D., Schmitzer-Osborne, S. E. & Naylor, C. E. Phosphate/calcium alterations in the first stages of Alzheimer's disease: Implications for etiology and pathogenesis. *J. Neurol. Sci.* **106**, 221–229 (1991).
10. Birnboim, H. C. & Doly, J. A rapid alkaline extraction procedure for screening recombinant plasmid DNA. *Nucleic Acids Res.* **7**, 1513–23 (1979).
11. Bon, N. *et al.* Phosphate (Pi)-regulated heterodimerization of the high-affinity sodium-dependent Pi transporters PiT1/Slc20a1 and PiT2/Slc20a2 underlies extracellular Pi sensing independently of Pi uptake. *J. Biol. Chem.* **293**, 2102–2114 (2018).
12. Katsnelson, A. Male researchers stress out rodents. *Nature* (2014). doi:10.1038/nature.2014.15106
13. Bartsch, T. & Wulff, P. The hippocampus in aging and disease: From plasticity to vulnerability. *Neuroscience* **309**, 1–16 (2015).
14. Grady, C. The cognitive neuroscience of ageing. *Nat. Rev. Neurosci.* **13**, 491–505 (2012).
15. Mizushima, N. Autophagy: process and function. *Genes Dev.* **21**, 2861–2873 (2007).
16. Rubinsztein, D. C., Mariño, G. & Kroemer, G. Autophagy and Aging. *Cell* **146**, 682–695 (2011).
17. Hirokawa, N., Sobue, K., Kanda, K., Harada, A. & Yorifuji, H. The cytoskeletal architecture of the presynaptic terminal and molecular structure of synapsin 1. *J. Cell Biol.* **108**, 111–26 (1989).
18. Kügler, S., Kilic, E. & Bähr, M. Human synapsin 1 gene promoter confers highly neuron-specific long-term transgene expression from an adenoviral vector in the adult rat brain depending on the transduced area. *Gene Ther.* **10**, 337–347 (2003).

<https://github.com/basile6/MouseTracking>